

RSC Advances



This is an *Accepted Manuscript*, which has been through the Royal Society of Chemistry peer review process and has been accepted for publication.

Accepted Manuscripts are published online shortly after acceptance, before technical editing, formatting and proof reading. Using this free service, authors can make their results available to the community, in citable form, before we publish the edited article. This *Accepted Manuscript* will be replaced by the edited, formatted and paginated article as soon as this is available.

You can find more information about *Accepted Manuscripts* in the [Information for Authors](#).

Please note that technical editing may introduce minor changes to the text and/or graphics, which may alter content. The journal's standard [Terms & Conditions](#) and the [Ethical guidelines](#) still apply. In no event shall the Royal Society of Chemistry be held responsible for any errors or omissions in this *Accepted Manuscript* or any consequences arising from the use of any information it contains.

Small Band Gap D- π -A- π -D Benzothiadiazole Derivatives Having Low Lying HOMO Levels as Potential Donors for Applications in Organic Photovoltaics: A Combined Experimental and Theoretical Investigation

Mahalingavelar Paramasivam ^{a, b}, Akhil Gupta ^c, Aaron M. Raynor ^c,

Sheshanth V. Bhosale ^{c, *}, K.Bhanuprakash ^{a, d, *} and V.Jayathirtha Rao ^{b, d, *}

^a Inorganic and Physical Chemistry Division, CSIR-Indian Institute of Chemical Technology, Hyderabad, 500007, India.

E-mail: bhanu2505@yahoo.co.in

^b Crop Protection Chemicals Division, CSIR-Indian Institute of Chemical Technology, Hyderabad, 500007 India.

E-mail: jrao@iict.res.in

^c School of Applied Sciences, RMIT University, GPO Box 2476V, Melbourne Victoria 3001 Australia.

E-mail: sheshanath.bhosale@rmit.edu.au

^d CSIR-Network of Institutes for Solar Energy, New Delhi, India.

Abstract

In this work, aiming for small organic molecules with potential applications as donors in organic photovoltaic (OPV) devices, we have synthesized and characterized four novel benzothiadiazole (A) core structured D- π -A- π -D dyes featuring carbazole, benzocarbazole as donors (D) and fluorene, thiophene as spacers (π). The effect of π -spacer units along with variations in donor strength on their photophysical, electrochemical and thermal properties have been investigated in detail. Replacement of fluorene by thiophene as a π -spacer promotes planarity which results in a larger bathochromic shift in absorption, emission profiles and enhanced intramolecular charge transfer (ICT) transition. The introduction of benzocarbazole unit creates a low lying HOMO level as inferred from cyclic voltammetry studies. All the dyes exhibit remarkable thermal robustness. Theoretical calculations have been carried out to understand structure-property relationship. The results obtained from the characterization methods reveal that the dyes with thiophene π -spacer show better optoelectronic properties compared to the fluorene counterparts.

Solution-processable bulk-heterojunction devices with a structure of ITO/PEDOT: PSS (38 nm)/active layer/Ca (20 nm)/Al (100 nm) were fabricated using materials investigated in this study as donors and (6, 6)-phenyl C₆₁-butyric acid methyl ester (PC₆₁BM) as an acceptor. Power conversion efficiency of 1.62% for the molecule with thiophene as a spacer and carbazole as donor/PC₆₁BM was achieved for the preliminary photovoltaic devices under simulated AM 1.5 illumination (100 mW cm⁻²).

Keywords: Organic Photovoltaics, benzocarbazole, DFT, benzothiadiazole, thiophene.

Introduction

The quest to produce clean and renewable energy by developing organic π -conjugated molecules for organic photovoltaic (OPV) applications has attracted intensive attention of researchers over the last few decades.¹ In the beginning, organic solar cells were prepared using polymers as light harvesting electron donors owing to their high optical density, optimized film morphology and other superior properties.² Nevertheless of having these unique features, polymers encountered the problem of polydispersity, variation in batch to batch reproducibility and hefty purification thus paving the way for small organic molecules as emerging alternatives.^{3,4} Initially small molecules as electron donors lagged behind the polymers due to their inferior photovoltaic performance, even though the former holds several advantages such as facile synthesis, well-defined molecular structures, and amenability for large scale production, etc. Later the efficiency of small molecule organic solar cells began to evolve gradually and have reached 8.2% by scrutinized molecular design.⁵ Recently, tandem solar cells featuring small molecules have been reported with the unprecedented cell efficiency of 12% on a

standard size of 1.1 cm² by Heliatek, a German company.⁶ Looking at this trend, the day may not be far off when small molecule organic solar cells will outperform polymer counterparts.

To improve the photovoltaic performance of small molecules there are many factors such as light absorption, charge carrier transport, carrier injection, charge separation, etc. that should be considered.⁷ An elegant way is to design these small molecules by the combination of various π -building blocks and utilize into the backbone structures, keeping in mind the following points 1) to improve the photocurrent (J_{sc}), small HOMO-LUMO gap of a molecule is necessary (without sacrificing V_{oc}); 2) control of frontier energy levels which are mostly dependent on the chemical structures of individual π -building blocks to match the electron acceptors energy levels such as [6, 6]-phenyl- C61-butyric acid methyl ester (PC₆₁BM), and perylenediimides (PDI) so as to facilitate the rate of electron injection efficiently. A very active area of research is bringing out novel small band gap molecules with low lying HOMOs as donors for OPV with D- π -A- π -D configuration.¹⁰⁻¹⁶ Recently, Zeng *et al.* introduced a cyano group on the spacer of benzothiadiazole-triphenylamine system thereby stabilizing the HOMO level to 5.32 eV.¹⁰ On the other hand, Cho *et al.* introduced the fluorine group on benzothiadiazole acceptor unit which resulted in an efficiency of 2.95%. This is due to high V_{oc} attributed to low HOMO level and retention of the band gap.¹¹ Tian and co-workers tuned the band gap of small molecules by the introduction of pyran-4-ylidenemalononitrile and electron-donating group TPA linked by different conjugation units and the enhancement in efficiency was obtained from the compounds having low lying HOMO values.¹² This principle was adopted by Sassi *et al.* to control the HOMO level by synthesizing a new series of end-capped diphenylhydrazone derivatives bearing a variety of electron withdrawing conjugated bridges with different substitution pattern.¹³ Romero *et al.* evaluated the band gap of the molecules by altering the acceptor strength from

fluorene, fluorenone to benzothiadiazole.¹⁴ As a result, the ICT character of the molecules was improved. Recently, Azoulay *et al.* have demonstrated the tuning of HOMO/LUMO energy levels by the incorporation of various bridgehead imine substituted cyclopentadithiophene derivatives along with benzothiadiazole core unit which influences the aromatic stabilization with unprecedented precision.¹⁵

Based on the above points, it would be of interest to develop the molecules which contain chromophores with high optical density. A deliberate functional group selection for modification of energy levels is essential so as to extend the absorption to cover the maximum range of solar spectrum.¹⁷ This also offers the possibility to probe the structure-property relationship and gain insight into the development of better candidates for solution-processable solar cells. Furthermore, optical and electrochemical properties could be fine-tuned by the appropriate inclusion of different π -spacers and donors into the π -conjugated backbone, which have been less explored to date.¹⁸ In recent years, numerous articles have been reported with small molecule electron donors containing different heterocycle units such as benzothiadiazole,^{5, 18} squaraines,¹⁹ diketopyrrolopyrrole²⁰ and tetrazine²¹ etc with inherent charge transfer nature. Among that, benzothiadiazole is considered as one of the versatile heterocycle units which has been extensively used to make enormous improvement in organic dyes for photovoltaic applications.²² High efficiency of 6.8% has been reported due to the good electron carrier propensity of thiadiazole moiety which leads to strong π - π interactions result in an ordered morphology with efficient charge transport and excellent thermal stability. The incorporation of such kind of electron deficient moiety into the π -conjugated system stabilizes the frontier energy levels and aligns with electron acceptor energy levels to achieve the optimized efficiency with minimized loss mechanism.

The purpose of this combined experimental and theoretical study is to explore the tuning of absorption and band gap in D- π -A- π -D conjugated backbone with insertion of different π -conjugated units and variation in donor strength. Our main design principle is to use benzothiadiazole core derivatives which are known to yield small band gaps with benzocarbazole/carbazole donors which have low lying HOMO levels. Herein, we report the synthesis and detailed characterization of four novel dyes based on D- π -A- π -D architecture comprising the molecular combinations of carbazole, benzocarbazole as donors, benzothiadiazole as central acceptor unit (A) with fluorene π -spacer denoted as CFBFC and BFBBFB respectively and thiophene π -spacer with the same donors are denoted as CTBTC and BTBTB respectively (Figure 1). Quantum chemical calculations have been used here as a guide for the analysis of the ground state and excited state properties.^{23, 24} The influence of π -spacers on different donors flanked with benzothiadiazole and their effect on photophysical and electrochemical properties have been investigated for these compounds which could help to design more efficient functional photovoltaic organic materials. We have compared the effect of benzocarbazole moiety with its congener carbazole group as donor along with different π -spacers. To improve the solubility and film morphology, an additional ethylhexyl group to the donors and butyl group to the fluorene moieties have been attached.

EXPERIMENTAL SECTION

Materials and General Procedures

Unless otherwise specified, all the reactions were performed under nitrogen atmosphere with standard Schlenk techniques. All the reagents in reagent/analytical grade and used without further purification. THF, toluene were distilled from sodium and benzophenone under nitrogen atmosphere. All chromatographic separations were carried out on silica gel (60-

120 mesh). ^1H NMR and ^{13}C NMR spectra were recorded on a Bruker Avance (300 MHz) spectrometer in CDCl_3 and DMSO-d_6 with TMS as standard in both cases. Mass spectra were obtained by using electron ionization (EI) mass spectrometry (ThermoFinnigan, Sanzox, CA), Gas Chromatography-Mass Spectrometry (GCMS) recorded on VG70–70H and MALDI-TOF Mass Spectrometry was obtained from Axima performance MALDI-TOF/TOF mass spectrometer (Shimadzu). UV–Vis absorption spectra were measured on a Perkin-Elmer spectrofluorometer and fluorescence spectra were recorded using a Spex model Fluorolog-3 spectrofluorometer. Perkin-Elmer Spectrum BX spectrophotometer was used to obtain IR spectra of the dyes at a resolution of 4 cm^{-1} . Thermo gravimetric analyses (TGA) were performed with a TGA/SDTA 851e (Mettler Toledo) thermal analyzer with a heating rate of $10^\circ\text{C min}^{-1}$ under nitrogen atmosphere in the temperature range of $33\text{--}550^\circ\text{C}$. The glass-transition temperatures (T_g) of the compounds were measured using differential scanning calorimetry (DSC) under a nitrogen atmosphere and at a heating rate of $10^\circ\text{C min}^{-1}$ using a DSC Q200 (TA instruments). The T_g was determined from the second heating scan. Melting points were measured with an Electro thermal IA 9100 series digital melting point instrument and are uncorrected. Cyclic voltammetric measurements were performed on a PC-controlled CH instruments model CHI 620C electrochemical analyzer, using 1 mM dye solution in dichloromethane (DCM) at a scan rate of 50 mV/s using 0.1 M tetra butyl ammoniumperchlorate (TBAP) as supporting electrolyte. The glassy carbon, standard calomel electrode (SCE) and platinum wire were used as working, reference and auxiliary electrodes respectively.

Device fabrication and characterization of photovoltaic devices

Indium tin oxide (ITO)-coated glass (Kintek, 15 Ohms/square) was cleaned by standing in a stirred solution of 5% (v/v) Deconex 12PA detergent at 90 °C for 20 min. The ITO-coated glass was then successively sonicated for 10 min each in distilled water, acetone, and isopropanol. The substrates were then exposed to a UV-ozone clean at room temperature for 10 min. UV/ozone cleaning of glass substrates was performed using a Novascan PDS-UVT, UV/ozone cleaner with the platform set to maximum height. The intensity of the lamp was greater than 36 mW/cm² at a distance of 10 cm. At ambient conditions, the ozone output of the UV cleaner is greater than 50 parts per million (ppm). Aqueous solutions of PEDOT/PSS (HC Starck, Baytron P AI 4083) were filtered (0.2 µm RC filter) and deposited onto glass substrates in air by spin coating (Laurell WS-400B-6NPP lite single wafer spin processor) at 5000 rpm for 60 s to give a layer having a thickness of 40 ± 5 nm. The PEDOT/PSS layer was then annealed on a hotplate in a glove box at 145 °C for 10 min. For OPV devices, the newly synthesized organic *p*-type materials and PC₆₁BM (Nano-C) were separately dissolved in individual vials by magnetic stirring. The solutions were then combined, filtered (0.2 µm RC filter), and deposited by spin coating (SCS G3P spin coater) onto the ITO-coated glass substrates inside a glove box (with H₂O and O₂ levels both <1 ppm). Film thicknesses were determined on identical samples using a Dektak 6M Profilometer. The coated substrates were then transferred (without exposure to air) to a vacuum evaporator inside an adjacent nitrogen-filled glove box. Samples were placed on a shadow mask in a tray. The area defined by the shadow mask gave device areas of exactly 0.2 cm². Deposition rates and film thicknesses were monitored using a calibrated quartz thickness monitor inside the vacuum chamber. Layers of calcium (Ca) (Aldrich) and aluminium (Al) (3 pellets of 99.999%, KJ Lesker) having thicknesses of 20 nm and 100 nm, respectively,

were evaporated from open tungsten boats onto the active layer by thermal evaporation at pressures less than 2×10^{-6} mbar. Where used, C₆₀ (Nano-C) and 2,9-dimethyl-4,7-diphenyl-1,10-phenanthroline (Aldrich) were evaporated from alumina crucibles. A connection point for the ITO electrode was made by manually scratching off a small area of the active layers. A small amount of silver paint (Silver Print II, GC Electronics, part number: 22-023) was then deposited onto all of the connection points, both ITO and Al. The completed devices were then encapsulated with glass and a UV-cured epoxy (Summers Optical, Lens Bond type J-91) by exposing to 365 nm UV light inside the glove box for 10 min. The encapsulated devices were then removed from the glove box and tested in air within 1 h. Electrical connections were made using alligator clips. The OPV devices were tested using an Oriel solar simulator fitted with a 1000 W xenon lamp filtered to give an output of 100 mW/cm² at simulated AM 1.5.²⁵ The lamp was calibrated using a standard, filtered silicon (Si) cell from Peccell Limited, which was subsequently cross-calibrated with a standard reference cell traceable to the National Renewable Energy Laboratory. The devices were tested using a Keithley 2400 source meter controlled by Lab-view software.

8-bromo-11H-benzo[a]carbazole (5)

α -Tetralone (9.16g, 6.26 mmol) and 4-bromophenylhydrazine hydrochloride (10 g, 44.7 mmol) were dissolved in 300 mL of ethanol, and then catalytic amount of acetic acid was added to the reaction mixture, refluxed for 3 hours under nitrogen atmosphere. The reaction mixture was cooled to room temperature; the formed product was filtered, dried and used for next step without purification. The dried compound (9.29 g, 30.8 mmol) and tetrachloro-1-benzoquinone (10.6 g, 43.2 mmol) in xylene were refluxed under nitrogen atmosphere for 8 hours, cooled to room temperature, NaOH (10%) and water were put into the reaction solution, the organic layer

was extracted with ethyl acetate and dried over sodium sulphate. The reaction solution was concentrated, purified by column chromatography over silica gel and the purified compound was recrystallized with ethanol to give desired product as white crystals (8.8 g, yield 96%). **¹H NMR (500 MHz, CDCl₃):** 8.24 (s, 1H), 8.23-7.99 (m, 3H), 7.68-7.44 (m, 5H). **¹³C NMR (125 MHz, CDCl₃):** 137.5, 132.6, 128.8, 127.0, 125.5, 125.4, 122.3, 121.6, 120.0, 119.1, 112.7. **GC/MS:** *m/z* 296 [M]⁺.

3-bromo-9-(2-ethylhexyl)-9H-carbazole (6a)

3-Bromo-9H-carbazole (5 g, 20.3 mmol), 2-ethylhexyl bromide (5.4 mL, 30.5 mmol), 50% aq.NaOH and catalytic amount of tetrabutylammonium iodide (0.75 g, 10 mol %) was taken in a flask. The reaction mixture was heated to 70⁰C continuously for 8 hrs, and then cooled to room temperature. The reaction mixture was extracted with hexane, washed with water and dried over anhydrous sodium sulphate. The solvent was removed under vacuum and the crude was purified by column chromatography over silica gel with *n*-hexane as the eluent to give the desired product as white solid (6.67 g, Yield 92%). **¹H NMR (500 MHz, CDCl₃):** 8.29 (s, 1H), 8.10-8.09 (d, 1H, *J*=7.9 Hz), 7.63-7.57 (d, 2H, *J*=8.9 Hz), 7.45-7.44 (d, 1H, *d*=7.9 Hz), 7.35-7.32 (t, 1H, *J*=14.9 Hz), 4.08-4.06 (m, 2H, N-CH₂), 2.12-2.09 (m, 1H), 1.46-1.38 (m, 8H), 1.38-0.76 (m, 6H). **¹³C NMR (125 MHz, CDCl₃):** 140.7, 138.9, 127.7, 125.8, 124.1, 122.4, 121.3, 119.9, 118.7, 111.1, 109.8, 108.7, 46.8, 38.8, 30.5, 28.5, 28.4, 23.9, 22.7, 13.7, 10.5. **GC/MS:** *m/z* 358 [M]⁺.

8-bromo-11-(2-ethylhexyl)-11H-benzo[a]carbazole (6b)

This compound was synthesized according to the procedure similar to that of 6a, using 8-bromo-11H-benzo[a]carbazole (5.0 g, 16.9 mmol), to give the desired product as white solid (6.4g, Yield 93%). **¹H NMR (500 MHz, CDCl₃):** 8.39 (d, 1H, *J* = 8.3 Hz), 8.16 (d, 1H, *J* = 2.3

Hz), 7.99 (d, 2H, $J = 8.3$ Hz), 7.60-7.44 (m, 4H), 7.28 (t, 1H, $J = 14.6$ Hz), 4.41-4.37 (m, 2H, N-CH₂), 2.17-2.13 (m, 1H, N-CH₂-CH), 1.52-1.16 (m, 8H), 0.91-0.78 (m, 6H). **¹³C NMR (125 MHz, CDCl₃):** 139.6, 134.9, 133.8, 129.5, 127, 125.2, 124.8, 124.3, 122.1, 122, 121, 118.8, 118.3, 112.2, 111.2, 49.9, 39.5, 28.4, 23.8, 23, 14, 10.7. **GC/MS:** m/z 408 [M]⁺.

9-(2-ethylhexyl)-3-(4, 4, 5, 5-tetramethyl-1, 3, 2-dioxaborolan-2-yl)-9H-carbazole (7a)

To a solution of 3-bromo-9-(2-ethylhexyl)-9H-carbazole (6a) (5 g, 14.1 mmol) in anhydrous THF (120 mL) at -78⁰C, of *n*-butyl lithium (2 M in hexane; 7.75 mL, 15.3 mmol) was added. The mixture was stirred at -78⁰C for 2 h. 3.25 mL of 2-isopropoxy-4, 4, 5, 5-tetramethyl-[1, 3, 2]-dioxaborolane (16.7 mmol) was added rapidly to the solution, and the resulting mixture was warmed to room temperature and stirred overnight. The mixture was poured into water and extracted with chloroform. The organic extracts were washed with brine, dried with anhydrous sodium sulphate. The solvent was removed by rotary evaporation, and purified by column chromatography over silica gel with *n*-hexane: ethyl acetate (95:5) as the eluent to give the desired product as white solid (5.1 g, Yield 89%). **¹H NMR (500 MHz, CDCl₃):** 8.64 (s, 1H), 8.12-8.10 (d, 1H, $J=8.3$ Hz), 7.95-7.92 (d, 1H, $J=8.3$ Hz), 7.38-7.15 (m, 4H), 3.92-3.89 (m, 2H, N-CH₂), 1.94 (m, 1H), 1.33 (s, 12H), 1.25-1.16 (m, 9H), 0.82-0.76 (t, 6H, $J=12.1$). **¹³C NMR (125 MHz, CDCl₃):** 143.2, 141.1, 132.4, 127.9, 125.8, 123.3, 122.8, 120.6, 119.4, 109.2, 108.6, 83.6, 47.3, 39.4, 31.1, 28.9, 25.1, 24.5, 23.2, 14.3, 11.1. **GC/MS:** m/z 405 [M]⁺.

11-(2-ethylhexyl)-8-(4, 4, 5, 5-tetramethyl-1, 3, 2-dioxaborolan-2-yl)-11H-benzo[a]carbazole (7b)

This compound was synthesized according to the procedure similar to that of 7a, using 8-bromo-11-(2-ethylhexyl)-11H-benzo[a]carbazole (5.0 g, 12.3 mmol), to give the desired product as white solid (5.3 g, Yield 95%). **¹H NMR (500 MHz, CDCl₃):** 8.66 (s, 1H), 8.52 (d, 1H, $J = 7.9$

Hz), 8.24 (d, 1H, $J = 3.9$ Hz), 8.02 (d, 1H, $J = 6.9$ Hz), 7.92 (d, 1H, $J = 7.9$ Hz), 7.68 (d, 1H, $J = 8.9$ Hz), 7.58 (m, 3H), 4.72-4.62 (m, 2H, N-CH₂), 2.28-2.24 (m, 1 H, N-CH₂-CH), 1.41(s, 12H), 1.37-1.16 (m, 8H), 0.86-0.80 (m, 6H). ¹³C NMR (125 MHz, CDCl₃): 142.4, 133.8, 132.8, 130.1, 128.8, 126.4, 124.3, 123.6, 121.8, 121.6, 121.3, 120.3, 119, 118.4, 108.4, 82.7, 82.6, 49, 38.8, 29.7, 27.7, 24.3 (4-CH₃), 23, 22.2, 13.2, 10. GC/MS: m/z 455 [M]⁺.

3-(7-bromo-9, 9-dibutyl-9H-fluoren-2-yl)-9-(2-ethylhexyl)-9H-carbazole (8a)

9-(2-Ethylhexyl)-3-(4, 4, 5, 5-tetramethyl-1, 3, 2-dioxaborolan-2-yl)- 9H-carbazole (7a) (4 g, 9.86 mmol), 2, 7-dibromo-9, 9-dibutyl-9H-fluorene (6) (5.17 g, 11.83 mmol) and tetrakis (triphenylphosphine) palladium(0) (115 mg, 0.001 mmol) were dissolved in the mixture of toluene and aqueous 2 M potassium carbonate solution (3:1, v/v) in a round-bottomed flask equipped with a reflux condenser and the reaction mixture was heated to 80°C for 24 h. The cooled reaction mixture was filtered, poured into water, extracted with chloroform and dried with anhydrous sodium sulphate. The solvent was removed by rotary evaporation and purified by column chromatography over silica gel with *n*-hexane as the eluent to give the desired product as white foamy solid. (4.6 g, 7.2 mmol, Yield 73%). ¹H NMR (500 MHz, CDCl₃): 8.37 (s, 1H), 8.16-8.14 (d, 1H, $J=7.7$ Hz), 7.72-7.49 (m, 4H), 7.44 (s, 1H), 7.41-7.18 (m, 7H), 4.02-4.00 (m, 2H, N-CH₂), 2.02-1.99 (m, 5H), 1.31-1.24 (m, 12H), 1.11-1.06 (m, 6H), 0.85-0.78 (m, 8H). ¹³C NMR (125 MHz, CDCl₃): 153.5, 151.4, 141.9, 141.7, 140.7, 140.4, 138.7, 132.7, 130.3, 129.1, 127.6, 127.6, 126.6, 126.4, 126.2, 125.5, 123.7, 123.3, 121.8, 121.3, 121.1, 120.8, 120.5, 119.3, 119.0, 109.5, 55.7, 47.6, 40.6, 39.7, 31.3, 29.2, 26.3, 26.3, 24.7, 23.4, 14.5, 14.2, 11.3. MS (EI): m/z 635 [M]⁺.

8-(7-bromo-9, 9-dibutyl-9H-fluoren-2-yl)-11-(2-ethylhexyl)-11H-benzo[a]carbazole (8b)

This compound was synthesized according to the procedure similar to that of 8a, using 8-bromo-11-(2-ethylhexyl)-11H-benzo[a]carbazole (4.0 g, 8.79 mmol), to give the desired product as white foamy solid. (4.2 g, 6.1 mmol, Yield 69%). **¹H NMR (500 MHz, CDCl₃):** 8.48 (d, 1H, *J* = 8.3 Hz), 8.38 (d, 1H, *J* = 1.5 Hz), 8.23 (d, 1H, *J* = 9.1 Hz), 7.98 (d, 1H, *J* = 8.31 Hz), 7.92 (d, 1H, *J* = 7.9 Hz), 7.74-7.63 (m, 4H), 7.57-7.42 (m, 5H), 4.60-4.45 (m, 2H, N-CH₂), 2.27-2.22 (m, 1H, N-CH₂-CH), 2.12-1.93 (m, 4H), 1.43-1.04 (m, 8H), 0.86-0.80 (t, 6H, *J* = 7.55), 0.72-0.67 (t, 6H, *J* = 8.31). **¹³C NMR (125 MHz, CDCl₃):** 153.2, 151.1, 141.6, 140.8, 140.1, 138.5, 135.2, 133.8, 133.1, 130.0, 127.6, 126.4, 126.2, 125.2, 124.6, 124.3, 123.4, 122.6, 122.2, 121.6, 121.0, 120.8, 120.7, 120.1, 119.7, 119.2, 117.9, 110.2, 55.5, 50.2, 40.3, 39.7, 30.6, 28.6, 26.0, 23.9, 23.1, 14.1, 13.9, 10.8. **MS (EI):** *m/z* 684 [M]⁺.

3-(9, 9-dibutyl-7-(4, 4, 5, 5-tetramethyl-1, 3, 2-dioxaborolan-2-yl)-9H-fluoren-2-yl)-9-(2-ethyl hexyl)-9H-carbazole (9a)

To a solution of 3-(7-bromo-9, 9-dibutyl-9H-fluoren-2-yl)-9-(2-ethylhexyl)-9H-carbazole (8a) (3 g, 4.7 mmol) in anhydrous THF (120 mL) at -78⁰C, 2.6 mL of *n*-butyl lithium (2 M in hexane; 5.2 mmol) was added. The mixture was stirred at -78⁰C for 2 h. 2-isopropoxy-4, 4, 5, 5-tetramethyl-[1, 3, 2]-dioxaborolane (1.15 mL, 5.64 mmol) was added rapidly to the solution, the resulting mixture was warmed to room temperature and stirred overnight. The reaction mixture was poured into water and extracted with chloroform. The organic extracts were washed with brine, dried with anhydrous sodium sulphate. The solvent was removed by rotary evaporation, and purified by column chromatography over silica gel with *n*-hexane: ethyl acetate (95:5) as the eluent to give the desired product as white solid (2.9 g, 4.25 mmol, Yield 90%). **¹H NMR (500 MHz, CDCl₃):** 8.59-8.55 (d, 2H, *J*=10.6 Hz), 8.37-8.34 (d, 1H, *J*=8.3 Hz), 7.66-7.61 (m, 3H), 4.61 (m, 2H, N-CH₂), 2.36-2.27 (m, 5H), 1.53 (s, 12H), 1.46-1.25 (m, 12H), 0.96-0.83 (m, 16H).

¹³C NMR (125 MHz, CDCl₃): 151.6, 149.7, 143.8, 141.3, 140.9, 139.9, 134.4, 133.6, 132.2, 128.5, 127.3, 126.8, 125.8, 125.4, 124.9, 123.0, 122.6, 121.1, 120.2, 120.0, 118.6, 118.3, 108.8, 108.7, 83.2, 54.8, 46.9, 40.0, 39.0, 30.6, 28.5, 26.6, 25.7, 24.6, 24.0, 22.8, 22.7, 13.8, 13.6, 10.6.

ESI-MS: *m/z* 683 [M]⁺.

8-(9, 9-dibutyl-7-(4, 4, 5, 5-tetramethyl-1, 3, 2-dioxaborolan-2-yl)-9H-fluoren-2-yl)-11-(2-ethylhexyl)-11H-benzo[a]carbazole (9b)

This compound was synthesized according to the procedure similar to that of 9a, using 8-(7-bromo-9, 9-dibutyl-9H-fluoren-2-yl)-11-(2-ethylhexyl)-11H-benzo[a]carbazole (3.0 g, 4.38 mmol), to give the desired product as white foamy solid. (2.8 g, 3.82 mmol, Yield 87%). **¹H NMR (500 MHz, CDCl₃):** 8.42-8.38 (d, 2H, J=10.6 Hz), 8.18-8.17 (d, 1H, J=8.3 Hz), 7.97-7.62 (m, 10H), 7.59-7.44 (m, 3H), 4.44-4.41 (m, 2H, N-CH₂), 2.12-2.09 (m, 5H), 1.36 (s, 12H), 1.29-1.08 (m, 12H), 0.82-0.79 (t, 6H), 0.70-0.66 (m, 10H). **¹³C NMR (125 MHz, CDCl₃):** 151.7, 149.8, 143.8, 141.3, 140.3, 139.1, 134.7, 133.6, 133.4, 132.8, 129.3, 128.6, 126.8, 125.9, 124.7, 124.2, 123.9, 122.9, 122.2, 121.9, 121.3, 120.4, 120.2, 119.3, 118.8, 118.7, 117.5, 109.8, 83.4, 54.9, 49.6, 40.1, 39.3, 30.3, 28.2, 25.7, 24.7, 23.6, 22.9, 22.7, 13.8, 13.6, 10.5. **MS (EI):** *m/z* 731 [M]⁺.

4, 7-bis (9, 9-dibutyl-7-(9-(2-ethylhexyl)-9H-carbazol-3-yl)-9H-fluoren-2-yl) benzo[c] [1, 2, 5] thiadiazole (CFBFC)

To a mixture of 3-(9,9-dibutyl-7-(4,4,5,5-tetramethyl-1,3,2-dioxaborolan-2-yl)-9H-fluoren-2-yl)-9-(2-ethylhexyl)-9H-carbazole (9a) (0.98 g, 1.43 mmol) and 4,7-dibromobenzo[c][1,2,5]thiadiazole (200 mg, 0.7 mmol) were dissolved in the mixture of toluene and aqueous 2 M potassium carbonate solution (3:1, v/v). Then tetrakis(triphenylphosphine) palladium (48 mg, 0.005 mmol) and 18 mol% of 18-crown-6 were added to the solution and degassed

with nitrogen for 15 minutes. The reaction mixture was heated at 80°C under nitrogen atmosphere for 24 h. The cooled reaction mixture was filtered, poured into water, extracted with chloroform, then dried over anhydrous sodium sulphate and evaporated to yield crude product. The residue was purified by column chromatography using hexane as the eluent to give the desired product **10** as yellow solid. (658mg, 0.53mmol, Yield 74%). **¹H NMR (500 MHz, CDCl₃):** 8.42 (s, 2H), 8.22-8.20 (d, 2H, J=7.7 Hz), 8.11-8.07 (d, 2H, J=7.9 Hz), 7.99 (s, 2H), 7.93-7.74 (m, 8H), 7.52-7.44 (m, 3H), 7.41-7.29 (m, 6H), 7.27-7.24 (m, 3H), 4.22-4.20 (m, 2H, N-CH₂), 2.16-2.12 (m, 10H), 1.54-4.38 (m, 20H), 0.89-0.76 (m, 12H). **¹³C NMR (125 MHz, CDCl₃):** 154.4, 152.0, 151.3, 141.4, 141.3, 141.2, 140.4, 139.1, 135.9, 133.5, 132.6, 128.2, 127.8, 126.2, 125.7, 125.2, 123.8, 123.3, 122.9, 121.6, 120.4, 120.2, 119.6, 118.7, 109.2, 109.1, 55.3, 47.5, 40.3, 39.5, 31.0, 28.9, 26.2, 24.4, 23.2, 23.0, 14.1, 13.9, 10.9. **MS (Maldi-TOF):** (m/z) Calcd: 1242.75; found: 1242.43.

4, 7-bis (9, 9-dibutyl-7-(11-(2-ethylhexyl)-11H-benzo[a]carbazol-8-yl)-9H-fluoren-2-yl) benzo[c][1, 2, 5]thiadiazole (BFBFB)

This compound was synthesized according to the procedure similar to that of **10**, using 8-(9, 9-dibutyl-7-(4, 4, 5, 5-tetramethyl-1, 3, 2-dioxaborolan-2-yl)-9H-fluoren-2-yl)-11-(2-ethylhexyl)-11H-benzo[a]carbazole (**9b**) (1.04 g, 1.43 mmol), with 2,7-dibromo benzothiadiazole (**2**) to give the desired product **11** as yellow solid. (600 mg, 0.45 mmol, Yield 62%). **¹H NMR (500 MHz, CDCl₃):** 8.51-8.46 (dd, 4H, J=22.9 Hz), 8.26-8.25 (d, 2H, J=5.3 Hz), 8.05-8.01 (m, 5H), 7.88-7.80 (m, 5H), 7.78-7.76 (m, 3H), 7.67-7.66 (d, 2H, J=6.4 Hz), 7.57-7.55 (d, 2H, J=6.3 Hz), 7.52-7.51 (d, 4H, J=8.3 Hz), 7.51-7.50 (m, 2H), 7.15 (s, 1H), 4.6-4.56 (m, 2H, N-CH₂), 2.30-2.18 (m, 10H), 1.46-1.38 (m, 24H) 1.29-1.18 (m, 19H) 0.86-0.76 (m, 12H). **¹³C NMR (125 MHz, CDCl₃):** 154.4, 152.0, 151.3, 141.3, 141.2, 140.7, 139.2, 135.9, 135.1, 133.7, 133.5, 129.6,

128.9, 128.2, 127.8, 126.3, 125.1, 124.5, 124.3, 123.9, 123.3, 122.5, 121.7, 120.7, 120.3, 119.6, 119.2, 117.8, 110.1, 55.3, 50.1, 40.3, 39.7, 30.6, 28.5, 26.2, 23.8, 23.2, 23.0, 14.0, 13.9, 10.8. **MS** (Maldi-TOF): (m/z) Calcd: 1342.78; found: 1342.43.

4, 7-bis (5-(9-(2-ethylhexyl)-9H-carbazol-3-yl) thiophen-2-yl) benzo[c][1, 2, 5]thiadiazole (CTBTC)

To a mixture of 9-(2-ethylhexyl)-3-(4,4,5,5-tetramethyl-1,3,2-dioxaborolan-2-yl)-9H-carbazole (7a) (0.93 g, 2.3 mmol) and 4,7-bis(5-bromothiophen-2-yl)benzo[c][1,2,5]thiadiazole (4) (500 mg, 1.1 mmol) were dissolved in the mixture of toluene and aqueous 2 M potassium carbonate solution (3:1, v/v). Then tetrakis(triphenylphosphine)palladium (63 mg, 0.005mmol) and 18 mol% of 18-crown-6 were added to the solution and degassed with nitrogen for 15 minutes. The reaction mixture was heated to 80°C under nitrogen atmosphere for 24 h. The cooled crude mixture was poured into water, extracted with chloroform, then dried over anhydrous sodium sulphate and evaporated to yield crude product. The residue was purified by column chromatography using hexane as the eluent to give the desired product 12 as black solid (587 mg, 0.69mmol, Yield 52%). **¹H NMR (500 MHz, CDCl₃):** 8.26 (m, 2H), 8.09-8.08 (d, 2H, J=7.2 Hz), 7.92 (m, 2H), 7.65-7.54 (m, 6H), 7.4-7.2 (m, 8H), 3.98 (m, 4H, N-CH₂), 1.98 (m, 2H), 1.50-1.23 (m, 16H), 0.86-0.83 (m, 12H). **¹³C NMR (125 MHz, CDCl₃):** 152.2, 146.6, 141.1, 137.1, 128.3, 125.7, 125.1, 124.9, 124.6, 123.6, 122.9, 122.5, 122.4, 120.2, 118.8, 117.3, 117.2, 109.0, 108.9, 47.2, 30.7, 28.5, 24.1, 22.3, 13.9, 13.8, 10.7. **MS** (Maldi-TOF): (m/z) Calcd: 854.38; found: 854.

4, 7-bis (5-(11-(2-ethylhexyl)-11H-benzo[a]carbazol-8-yl) thiophen-2-yl) benzo[c] [1, 2, 5]thiadiazole (BTBTB)

This compound was synthesized according to the procedure similar to that of 12, using 11-(2-ethylhexyl)-8-(4, 4, 5, 5-tetramethyl-1, 3, 2-dioxaborolan-2-yl)-11H-benzo[a]carbazole (7b) (1.04 g, 2.3 mmol), with 4,7-bis(5-bromothiophen-2-yl)benzo[c][1,2,5]thiadiazole (4) to give the desired product 13 as brown solid (632 mg, 0.66mmol, Yield 59%). **¹H NMR (500 MHz, CDCl₃):** 8.48-8.40 (m, 4H), 8.19-8.17 (m, 2H), 8.08-8.02 (m, 4H), 7.81-7.46 (m, 12H), 7.43-7.08 (m, 2H), 4.56 (m, 4H, N-CH₂), 2.23 (m, 2H), 1.55-1.24 (m, 16H), 0.86-0.84 (m, 12H). **MS (Maldi-TOF):** (m/z) Calcd: 954.38; found: 954.

Computational details

Density Functional Theory (DFT) calculations were performed using Gaussian 09 *ab initio* quantum chemical software package.²⁶ DFT has been used for the ground-state properties, and time-dependent DFT (TDDFT) for the estimation of ground to excited-state transitions. The optimized geometries for all of the molecules in their stable conformations with subsequent frequency calculations obtained using B3LYP/6-311G (d, p) level²⁷⁻²⁹ were used as the input for further calculations. To expedite the calculations without compromising the results, methyl groups were introduced instead of the solubilizers such as 2-ethylhexyl group in carbazole and benzocarbazole moieties and two butyl groups in fluorene. The geometries were then used to obtain the frontier molecular orbitals (FMOs) and also subjected to the single-point TDDFT studies (first 15 vertical singlet–singlet transitions) to obtain the UV-Vis spectra of the dyes. The integral equation formalism polarizable continuum model (PCM)^{30, 31} within the self-consistent reaction field (SCRF) theory, has been used for TDDFT calculations to describe the solvation of the dyes in chloroform solvent. The TDDFT calculations were performed with various functionals like B3LYP, PBE and M06-2X. The software GaussSum 2.2.5 was employed to simulate the major portion of the absorption spectrum and to interpret the nature of transitions.³²

The percentage contributions of individual units present in the dyes to the respective molecular orbitals were calculated.

Results and discussion

Synthesis of dyes

The target dyes CFBFC, BFBFB, CTBTC and BTBTB were synthesized according to a multistep synthetic pathway as illustrated in scheme 1. *o*-Phenylenediamine was treated with thionyl chloride to get benzothiadiazole (1), the subsequent bromination of 1 with bromine in 47% HBr solution provided the key intermediate 4,7-dibromo benzothiadiazole (2).³³ Then 2 was coupled with 2-tributylstannyl thiophene in presence of Pd(PPh₃)₄ under Stille conditions to get 4, 7-di(thiophen-2-yl) benzo[c][1, 2, 5]thiadiazole (3) and further bromination with *N*-bromosuccinimide gave 4,7-bis(5-bromo thiophen-2-yl)benzo[c][1,2,5]thiadiazole(4).³⁴ Synthesis of 8-bromo-11H-benzo[a] carbazole (5) was carried out according to Bücherer carbazole synthesis in two steps.³⁵ *N*-alkylation of 3-bromo-9H-carbazole, 8-bromo-11H-benzo[a] carbazole by 2-ethylhexyl bromide to yield 3-bromo-9-(2-ethylhexyl)-9H-carbazole (6a) and 8-bromo-11-(2-ethylhexyl)-11H-benzo[a]carbazole(6b) and C-dialkylation of 2, 7-dibromofluorene by 1-bromo butane to 2, 7-dibromo-9, 9'-dibutyl fluorene were synthesized according to the modified literature procedures.³⁶ The *N*-alkylated bromo derivative of carbazole (6a) and benzo[a]carbazole (6b) was treated with *n*-BuLi to eliminate the halogen atom at -78⁰C, and 2-isopropoxy-4, 4, 5, 5- tetramethyl-1, 3, 2-dioxaborolane was added to yield the corresponding boronate derivatives 7a and 7b.³⁷ The syntheses of bromo derivatives 8a and 8b were obtained in good yields by the Suzuki coupling of 2, 7-dibromo-9, 9'-dibutyl fluorene³⁸ with intermediates 7a and 7b in the presence of Pd(Ph₃)₄ as catalyst. The corresponding bromo derivatives 8a and 8b again boronated by following the same procedure used to prepare the intermediate 7a and 7b and

afford 3-(9, 9-dibutyl-7-(4, 4, 5, 5-tetramethyl-1, 3, 2-dioxaborolan-2-yl)-9H-fluoren-2-yl)-9-(2-ethylhexyl)-9H-carbazole (9a), 8-(9, 9-dibutyl-7-(4, 4, 5, 5-tetramethyl-1,3,2-dioxaborolan-2-yl)-9H-fluoren-2-yl)-11-(2-ethylhexyl)-11H-benzo[a]carbazole (9b). Finally, the dyes CFBFC, BFBBFB based on fluorene π -spacer were obtained through Suzuki coupling of 9a and 9b with 4, 7-dibromo benzo[c][1, 2, 5]thiadiazole (2) and the dyes CTBTC, BTBTB were obtained from the coupling of 8a and 8b with 4, 7-bis(5-bromothiophen-2-yl) benzo[c][1, 2, 5]thiadiazole (4) under the same reaction conditions.³⁹ All these molecules have been characterized by ¹H NMR, ¹³C NMR, IR, and EI-MS. MALDI-TOF mass spectrometry showed a molecular ion at the correct mass for the target dyes. The details of the experimental characterization data are available in the ESI.

Molecular Geometry and orbitals of the dyes

Theoretical investigation of the molecular geometries and the electron density distribution of the organic dyes is carried out to gain insight into these π -conjugated spacers and their effect on electronic and spectroscopic properties. An important aspect to be looked into is the planarity of the backbone to assess the degree of π -orbital overlap for efficient electron transport.⁴⁰ Due to the rotational freedom of the molecule, we obtain many local minima with very little energy difference. This indicates that the molecules may not have single dominant conformation in both solution and solid phase. To obtain the molecular orbital (MO) picture and vertical transitions, we freeze it in one local minima and carry out further studies including TDDFT (Figure 2).⁴¹ Variation of the vertical transition with respect to change in angle is investigated.

The electronic energies of the frontier molecular orbitals, used to assess the nature of charge transfer, and the isodensity plots of HOMO and LUMO for the four dyes are presented in

Figure 3. The HOMO is quite delocalized all over the spacer, acceptor and to an extent on the donor part. The electron density on terminal part of donors such as phenyl group in carbazole and naphthyl group in benzocarbazole is localized to lesser extent, which indicates that these moieties are not actively engaged in electron distribution as reflected in computed excitation energy of the dyes. The LUMO is mainly located on the central benzothiadiazole acceptor moiety and a little extent on adjacent electron rich thiophene rings in the thiophene derivatives. The similar pattern is observed for fluorene dyes also. The percentage contribution of each segments in the dyes have been computed from the frontier molecular orbitals such as HOMO, LUMO by dividing into three segments such as donor (D), π -spacer (P), and acceptor (A) using GaussSum software. The diagram is illustrated in figure S3, ESI.

Optical Properties

Evaluation of optical properties is essential to understand the small molecules applicability for optoelectronic devices. Figure 4 depicts the UV-Visible absorption and emission spectra of the four dyes CFBFC, BFBFB, CTBTC and BTBTB in chloroform solution and the corresponding optical properties are compiled in table 1. All the compounds showed two absorption bands which are characteristics of donor-acceptor based system. Among that, the higher energy absorption band at 320-370 nm corresponds to the localized π - π^* transition of the conjugated backbone. The intensity of π - π^* transition peaks for the fluorene dyes are relatively high. Dyes based on fluorene π -spacer such as CFBFC, BFBFB display the lower energy absorption band at 382-516 nm with the molar extinction coefficient of $\sim 3.5 \times 10^4 \text{ M}^{-1} \text{ cm}^{-1}$ which is ascribed to the intramolecular charge transfer (ICT) transition from the donor segments to acceptor group.⁴²⁻⁴⁴ The longer wavelength absorption maxima of 433 nm in BFBFB, comprising benzocarbazole as donor is almost identical to that of CFBFC (434 nm), the

carbazole counterpart which indicates that the introduction of different kind of donors such as carbazole, benzocarbazole has less pronounced effect on intramolecular charge transfer (ICT) for fluorene based dyes. It is important to note that, in comparison to the absorption spectra of fluorene based analogues, compounds based on thiophene π -spacer such as CTBTC, BTBTB exhibit two distinct absorption maxima at 524 nm and 499 nm respectively. The substitution of thiophene in place of fluorene leads to 65-90 nm bathochromic shift in the absorption and the emission profile as well. Additionally, the dye BTBTB which contains benzocarbazole as donor displays hyperchromic and hypsochromic effects when compared to the CTBTC.⁴⁵ It has been noticed that the area of ICT band of thiophene dyes (~ 250 nm) are almost twofold broad in comparison to that of fluorene dyes (~ 136 nm) and the intensity is also comparatively high, which implies that the ICT character of the dyes are enhanced by replacing the spacer units of fluorene by thiophene. In the film state, the absorption spectra exhibit an apparent broadening and bathochromic shift of absorption bands corresponding to that of the solution spectra due to the well structured and intermolecular interactions in the solid state.⁴⁶ Thus, the replacement of fluorene π -spacer by thiophene leads to 1) considerable reduction in band gap with large extension in spectral response which indicates that thiophene as π -spacer has effective electronic communication between donor and acceptor 2) extensive delocalization of thiophene dyes which lead to bathochromic shift due to the more planar conformation and high lying π -orbital along with smaller aromatic resonance energy of thiophene entity compared to fluorene.^{47, 48}

To further investigate the effect of solvent-solute interaction on the ICT character of the dyes, the absorption spectra was recorded in various solvents. The UV-Vis absorption and emission spectra of CTBTC recorded in various solvents are shown in Figure 5 and remaining dyes are shown in ESI. All these dyes showed negligible response to the solvent polarity for

intramolecular charge-transfer in the ground state.⁴⁹ In contrast, emission spectra of the dyes red shifted remarkably as polarity of the solvent increases. It is clear from that, in the presence of polar solvent, the non-polar locally excited (LE) state as seen in absorption is transformed into a polar excited state as seen from emission.⁵⁰ A distinct solvatochromic effect is observed for the thiophene derivatives rather than fluorene dyes. For example, emission maximum λ_{\max} of CTBTC is red-shifted from 644 nm in hexane to 712 nm in DMF which implies that the excited state of the compounds is well stabilized upon increasing the polarity of the solvent and displays red shifted emission. The large Stokes shift observed for fluorene dyes reveal that, these dyes undergo more structural relaxation during photoexcitation.⁵¹ The optical band gap (E_g) (Table 1) has been derived from the onset absorption spectra of the dyes in thin film state.

Based on the experimental observations and to have a deeper understanding of the excited-state transitions, TDDFT studies have been carried out for these molecules using different energy functionals such as B3LYP, PBE and M06-2X with 6-311G (d, p) basis set.^{52,53} The transition energies obtained in gas phase using the B3LYP and PBE functional are highly overestimated compared to the experimental results. On the other hand the absorption spectra computed using M06-2X gas phase results show only a small underestimation and this functional further used in the framework of Polarizable Continuum Model (PCM) with chloroform as the solvent. This is in reasonable agreement with the experimental values. Table 2 contains computed vertical excitation along with their oscillator strength, frontier orbital energies and compositions of vertical transitions in terms of molecular orbitals of all the dyes. The ground state and transition dipole moment of the dyes computed from DFT and TDDFT calculations also corroborate the experimental observation. The intramolecular charge transfer excited state is clearly formed from the HOMO to LUMO transition. It is evidently demonstrated that, the

percentage contribution of thiophene as π -spacer is superior to fluorene with regard to the electronic properties of the molecule which may be attributed to the effective orbital mixing over the whole π -conjugated system (Figure S3, ESI).^{8b}

To ascertain the charge transfer nature of π -spacers of the dyes upon photoexcitation, we have performed the absorption studies as a function of dihedral angle by varying from 0° to 60° in steps of 5° between the donor vs. π -spacer and π -spacer vs. acceptor in both the fluorene and thiophene derivatives using TDDFT calculations.^{54, 55} The structures used for this calculation have been obtained from the optimized geometry at B3LYP/6-311G (d, p) level. The absorption values obtained for these two derivatives with different position are plotted against dihedral angle are displayed in ESI (figures S5 and S6). It is clearly seen from the figures, the deviation of dihedral angle between the donor and π -spacer has pronounced effect on the absorption of BTBTB which leads to 45 nm bathochromic shift, whereas only 11 nm redshift is observed in the case of BFBFB. The dye BTBTB exhibits fourfold variation in absorption substantiates that the thiophene as π -bridge unit promotes the electron transport efficiently over the entire molecule. The variation of absorption in terms of dihedral angle deviation between the spacer and acceptor for these molecules are almost same (~ 97 nm).

Electrochemical studies

In order to evaluate electrochemical properties of these dyes, the redox behavior was investigated by performing the cyclic voltammetric (CV) technique with a standard three-electrode configuration.⁵⁴ The oxidation potentials in voltammograms reveal that all compounds undergo irreversible oxidation (Figure 6). The HOMO levels of all the compounds, calculated from the onset oxidation potential according to an empirical formula [$E_{\text{HOMO}} = -e(E_{\text{ox}} + 4.4)$ (eV)], and the LUMO levels, estimated from the onset reduction potentials⁵⁵ according to an

empirical formula [$E_{\text{LUMO}} = -e(E_{\text{red}} + 4.4)$ (eV)], are compiled in table 3. The onset oxidation potentials of the fluorene dyes BFBFB, CFBFC and the thiophene dyes BTBTB, CTBTC are estimated to be 1.35 V, 1.27 V, 1.13 V and 0.92 V corresponding to the HOMO levels of -5.75 eV, -5.67 eV, -5.53 eV, and -5.32 eV respectively. Among these compounds, BFBFB and BTBTB show more positive shift in oxidation potential implying that the incorporation of benzocarbazole moiety has significant effect on lowering the HOMO level corresponding to that of carbazole counterpart. This should also improve the V_{oc} (because V_{oc} is proportional to the energy difference between the HOMO of electron donor and the LUMO of electron acceptor in small molecule organic solar cells).^{45b} The onset reduction potentials of the dyes are estimated to be -1.12 V, -1.17 V, -0.95 V and -0.97 V corresponding to the LUMO levels of -3.28 eV, -3.23 eV, -3.45 eV and -3.43 eV respectively. It has been noticed that, the introduction of thiophene as π -spacer in place of fluorene leads to a reduction in the band gap and the HOMO and LUMO levels shift upwards and downwards by 0.22 eV, 0.17 eV respectively for BTBTB compared to BFBFB and 0.35 eV, 0.19 eV respectively for CTBTC compared to CFBFC as depicted in figure 7. The band gap reduces in the order of BFBFB (2.47 eV) > CFBFC (2.44 eV) > BTBTB (2.08 eV) > CTBTC (1.90 eV). The HOMO-LUMO gaps (ΔE) derived from cyclic voltammetry (CV) are in good agreement with the optical band gaps which are determined from the onset absorption spectra in thin film state. The DFT calculated HOMO and LUMO values are estimated to be -5.25 eV, -2.7 eV for fluorene derivatives and -5.04 eV, -2.9 eV for thiophene derivatives respectively follow the experimental trend. The HOMO-LUMO gap decreases gradually by the substitution of thiophene as π -spacer in place of fluorene. The HOMO-LUMO gap calculated from the frontier orbital energy values are estimated to be 2.5 eV and 2.4 eV for fluorene and 2.0 eV and 1.9 eV for thiophene derivatives respectively. These values are in

reasonably good agreement with the estimated electrochemical and optical band gap data. The band gaps using hybrid functionals with fully periodic boundary conditions (PBC) usually are known to give better agreement with the experimental results.⁵⁶

Thermal properties

The thermal properties of the four dyes were investigated by thermogravimetric analysis (TGA) and differential scanning calorimetry (DSC) under a nitrogen atmosphere at a heating rate of $10^{\circ}\text{C min}^{-1}$. The TGA analysis depicted in Figure 8, reveals that the 5% weight loss temperatures (T_d) of the dyes are ranging from $372\text{-}433^{\circ}\text{C}$. The melting points (T_m), glass-transition temperatures (T_g) were measured by carrying out DSC in N_2 atmosphere. The T_g and T_m values of benzocarbazole dyes are comparatively higher than the carbazole dyes, as seen from figure 9 and table 1. The T_g values are in the range of $63\text{-}124^{\circ}\text{C}$, determined from the second heating scan. It is apparently seen from the figures, fluorene analogues exhibits more thermal stability than their thiophene counterparts owing to the presence of rigid structural unit of fluorene.⁵⁷ All the dyes have good thermal stability, which is very essential for device fabrication process and other kinds of applications.

Photovoltaic properties

Because of their appropriate optoelectronic features, solubility and good film forming capabilities, all the materials were incorporated as p-type semiconducting components with the soluble fullerene derivative such as [6,6]-phenyl- C_{61} -butyric acid methyl ester (PC_{61}BM) as n-type semiconductor in bulk-heterojunction (BHJ) photovoltaic devices. BHJ architectures typically deliver higher device power conversion efficiencies by maximizing the surface area of the interface between the donor and acceptor materials in the active layer. For all the compounds, the device structure used was ITO/PEDOT: PSS (38 nm)/active layer/Ca (20 nm)/Al (100 nm)

where the active layer was a solution-processed blend of any of the donor materials reported here and the solubilized fullerene PC₆₁BM. This was done by spin coating mixtures of the appropriate dye with PC₆₁BM in chlorobenzene under ambient conditions in 1: 1 ratios without subsequent annealing. The optimum layer thickness was found to be in the range of about 70 nm. The best photovoltaic devices based on compound CTBTC gave a power conversion efficiency (η) of 1.62%. The respective current-voltage ($J-V$) curves are shown in Fig. 10.

The relatively lower efficiency achieved by using BFBFB, CFBFC and BTBTB than the CTBTC is likely due to the weaker absorption of the visible spectrum. This suggests that light harvesting ability of the small molecule donors plays an important role to achieve optimum photovoltaic performance. The modest fill factors observed for all devices suggest that the pathways for charge carriers to the electrodes are not optimized, a problem that could be addressed by using donor fragments that encourage stronger intermolecular interactions. With regards to the processing conditions of blend solutions, previous studies⁵⁸ indicate that there exists a strong effect of solvent and the degree of crystallization on the cell performance. Our attempts to fabricate the devices using low boiling solvent, such as chloroform, resulted in very poor photovoltaic performance. This was primarily due to poor film quality. The finding that the OPV devices comprising these novel donor materials perform better with high-boiling solvents is significant as the use of high-boiling solvents is preferable from a processing point of view. Table 4 represents the comparative photovoltaic performance data.

This preliminary study has been conducted using C₆₀-derivative of PCBM, however reports of using C₇₀-derivative for the enhancement of efficiency is mainly attributed to enhanced absorption in the film. Latter might be useful for the device optimization using materials reported in this study and is a work of near future.

Conclusion

In summary, we have reported four benzothiadiazole core structured compounds based on D- π -A- π -D architecture featuring different π -spacers of fluorene and thiophene along with benzocarbazole and carbazole as donors. The significance of these modifications on the individual segments of the dyes has been thoroughly investigated by using a range of experimental techniques such as optical, electrochemical and thermal methods. The enhanced oxidative and thermal stability of compounds BFBFB and BTBTB indicate that benzocarbazole functionality can play a vital role as donor for optoelectronic applications. The substitution of thiophene as π -spacer in place of fluorene has pronounced effect on their photophysical and electrochemical properties. The electrochemical bandgap of these dyes are greatly reduced by changing the π -spacer from fluorene to thiophene. The band gap derived from electrochemical studies is in good agreement with the band gap data derived from optical methods. From the electronic structure obtained from DFT methods, it is clear that the better performance of thiophene as π -spacer is largely due to the planarity of the molecule. The results obtained from thermal methods clearly establish that all the compounds have high decomposition temperatures (T_d) in the range of 372 - 435⁰C. The significant electronic and optical properties demonstrated by these dyes allowed us to fabricate them in solution processable BHJ OPV devices. After the preliminary device examination, the devices with CTBTC as donor material exhibit the best efficiency (1.62%) with PC₆₁BM. The inferior performance from rest of the materials is likely related to the weaker absorption in the visible region. Our results not only enrich the molecule library of the donors, but also point out that consideration of factors such as (1) light-harvesting, (2) charge carrier mobility and (3) solvent selection is pivotal in the design of the small molecule

donors. Further examination of the device fabrication using C₇₀-derivative of PCBM is the subject of on-going work in our laboratories.

Acknowledgements

MP thanks UGC for the fellowship. We thank the Director, CSIR-IICT for the encouragement. We acknowledge funding from NWP-0054 project. SVB acknowledges Australian Research Council under a Future Fellowship Scheme (FT110100152) and the School of Applied Sciences (RMIT University) provides the facilities.

References

1. a) Y. J. Cheng, S. H. Yang, and C. S. Hsu, *Chem. Rev.*, 2009, **109**, 5868–5923; b) B. C. Thompson and J. M. J. Fréchet, *Angew. Chem. Int. Ed.*, 2008, **47**, 58–77; c) C. Duan, F. Huang and Y. Cao, *J. Mater. Chem.*, 2012, **22**, 10416; d) Y. Li, *Acc.Chem.Res.*, 2012, **45**, 723-733.
2. a) P. Heremans, D. Cheyns, and B. P. Rand, *Acc.Chem.Res.*, 2009, **42**, 1740-1747; b) R. Kroon, M. Lenes, J. C. Hummelen, P. W. M. Blom, and B. De Boer, *Polymer Reviews*, 2008, **48**, 531–582; c) E. Bundgaard, and F. C. Krebs, *Solar Energy Materials & Solar Cells*, 2007, **91**, 954–985; d) C. L. Chochos, and S. A. Choulis, *Progress in Polymer Science*, 2011, **36**, 1326–1414; e) N. Blouin and M. Leclerc, *Acc.Chem.Res.*, 2008, **41**, 1110-1119.
3. a) A. Mishra and P. Bäuerle, *Angew. Chem. Int. Ed.*, 2012, **51**, 2020 – 2068; b) Y. Lin, Y. Li and X. Zhan, *Chem. Soc. Rev.*, 2012, **41**, 4245–4272; c) B. Walker, C. Kim, and T. Q. Nguyen, *Chem. Mater.*, 2011, **23**, 470–482.
4. a) Y. Chen, X. Wan, and G. Long, *Acc.Chem.Res.*, 2013, **46**, 2645-2655; b) F. Zhang, D. Wu, Y. Xu and X. Feng, *J. Mater. Chem.*, 2011, **21**, 17590; c) Z. B. Henson, K. Müllen and G. C. Bazan, *Nature Chemistry*, 2012, **4**, 699-704; d) J. E. Coughlin, Z. B. Henson, G. C. Welch, and G. C. Bazan, *Acc.Chem.Res.*, 2014, **47**, 257-270.
5. a) J. Zhou, Y. Zuo, X. Wan, G. Long, Q. Zhang, W. Ni, Y. Liu, Z. Li, G. He, C. Li, B. Kan, M. Li, and Y. Chen, *J. Am. Chem. Soc.*, 2013, **135**, 8484–8487; b) J. Zhou, Y. Zuo, X. Wan, Y. Liu, Y. Zuo, Z. Li, G. He, G. Long, W. Ni, C. Li, X. Su, and Y. Chen, *J. Am. Chem. Soc.*, 2012, **134**, 16345–16351; c) T. S. Van der Poll, J. A. Love, T. Q. Nguyen, and G. C. Bazan, *Adv.Mater.*, 2012, **24**, 3646-3649; d) A. K. K. Kyaw, D. H. Wang, V.

- Gupta, J. Zhang, S. Chand, G. C. Bazan, and A. J. Heeger, *Adv. Mater.*, 2013, **25**, 2397–2402.
6. http://www.heliatek.com/newscenter/latest_news/neuer-weltrekord-fur-organische-solarzellen-heliatek-behauptet-sich-mit-12-zelleffizienz-als-technologiefuhrer/?lang=en
7. a) H. Spanggaard, and F. C. Krebs, *Solar Energy Materials & Solar Cells*, 2004, **83**, 125–146; b) J. L. Brédas, J. E. Norton, J. Cornil, and V. Coropceanu, *Acc.Chem.Res.*, 2009, **42**, 1691-1699; c) J. Roncali, *Chem. Rev.*, 1997, **97**, 173-205.
8. a) L. Pandey, C. Risko, J. E. Norton, and J. L. Brédas, *Macromolecules*, 2012, **45**, 6405–6414; b) K. Takimiya, I. Osaka and M. Nakano, *Chem. Mater.*, 2014, **26**, 587–593; c) E. Kozma, M. Catellani, *Dyes and Pigments*, 2013, **98**, 160-179.
9. C. He, Q. He, X. Yang, G. Wu, C. Yang, F. Bai, Z. Shuai, L. Wang and Y. Li, *J. Phys. Chem. C*, 2007, **111**, 8661-8666.
10. S. Zeng, L. Yin, C. Ji, X. Jiang, K. Li, Y. Li and Y. Wang, *Chem. Commun.*, 2012, **48**, 10627–10629.
11. N. Cho, K. Song, J. K. Lee and J. Ko, *Chem. Eur. J.*, 2012, **18**, 11433 – 11439.
12. Z. Li, J. Pei, Y. Li, B. Xu, M. Deng, Z. Liu, H. Li, H. Lu, Q. Li and W. Tian, *J. Phys. Chem. C*, 2010, **114**, 18270–18278.
13. M. Sassi, M. Crippa, R. Ruffo, R. Turrisi, M. Drees, U. K. Pandey, R. Termine, A. Golemme, A. Facchetti and L. Beverina, *J. Mater. Chem. A*, 2013, **1**, 2631–2638.
14. J. R. Romero, L. A. Ixta, M. Rodríguez, G. R. Ortíz, J. L. Maldonado, A. J. Sánchez, N. Farfán, R. Santillan, *Dyes and Pigments*, 2013, **98**, 31-41. b) S. Tang, B. Li, and J. Zhang, *J. Phys. Chem. C*, 2013, **117**, 3221–3231.

15. J. D. Azoulay, Z. A. Koretz, B. M. Wong, and G. C. Bazan, *Macromolecules* 2013, **46**, 1337–1342.
16. a) Y. Liu, Y. M. Yang, C. Chen, Q. Chen, L. Dou, Z. Hong, G. Li, and Y. Yang, *Adv. Mater.*, 2013, **25**, 4657–4662;
17. A. Marrocchi, F. Silvestri, M. Seri, A. Facchetti, A. Taticchi and T. J. Marks, *Chem. Commun.*, 2009, 1380–1382.
18. a) B. A. D. Neto, A. A. M. Lapis, E. N. S. Júnior, and J. Dupont, *Eur. J. Org. Chem.*, 2013, **2**, 228-255; b) S. Xue, S. Liu, F. He, L. Yao, C. Gu, H. Xu, Z. Xie, H. Wu and Y. Ma, *Chem. Commun.*, 2013, **49**, 5730—5732.
19. a) L. Beverina and P. Salice, *Eur. J. Org. Chem.*, 2010, 1207–1225; b) L. Beverina, M. Drees, A. Facchetti, M. Salamone, R. Ruffo, and G. A. Pagani, *Eur. J. Org. Chem.*, 2011, 5555–5563; c) F. Silvestri, M. D. Irwin, L. Beverina, A. Facchetti, G. A. Pagani, and T. J. Marks, *J. Am. Chem. Soc.*, 2008, **130**, 17640–17641; d) D. Bagnis, L. Beverina, H. Huang, F. Silvestri, Y. Yao, H. Yan, G. A. Pagani, T. J. Marks, and A. Facchetti, *J. Am. Chem. Soc.*, 2010, **132**, 4074–4075.
20. a) S. Qu and H. Tian, *Chem. Commun.*, 2012, **48**, 3039–3051; b) B. Walker, A. B. Tamayo, X. D. Dang, P. Zalar, J.H. Seo, A. Garcia, M. Tantiwivat, and T. Q. Nguyen, *Adv. Funct. Mater.*, 2009, **19**, 3063–3069.
21. a) Y. Chen, C. Li, P. Zhang, Y. Li, X. Yang, L. Chen, Y. Tu, *Organic Electronics*, 2013, **14**, 1424-1434; b) Z. Li, J. Ding, N. Song, J. Lu, and Y. Tao, *J. Am. Chem. Soc.*, 2010, **132**, 13160–13161.
22. a) L. Lin, Y. Chen, Z. Huang, H. Lin, S. Chou, F. Lin, C. Chen, Y. Liu, and K. Wong, *J. Am. Chem. Soc.*, 2011, **133**, 15822–15825; b) Y. Chen, L. Lin, C. Lu, F. Lin, Z. Huang,

- H. Lin, P. Wang, Y. Liu, K. T. Wong, J. Wen, D. J. Miller, and S. B. Darling, *J. Am. Chem. Soc.*, 2012, **134**, 13616–13623.
23. a) N. Metri, X. Sallenave, C. Plesse, L. Beouch, P. H. Aubert, F. Goubard, C. Chevrot and G. Sini, *J. Phys. Chem. C*, 2012, **116**, 3765–3772; b) J. Zapala, M. Knor, T. Jaroch, A. M. Niedbala, E. Kurach, K. Kotwica, R. Nowakowski, D. Djurado, J. Pecaut, M. Zagorska, and A. Pron, *Langmuir*, 2013, **29**, 14503–14511; c) L. Sun, F. Bai, Z. Zhao, and H. Zhang, *Solar Energy Materials & Solar Cells*, 2011, **95**, 1800–1810.
24. a) N. M. O’Boyle, C. M. Campbell, and G. R. Hutchison, *J. Phys. Chem. C*, 2011, **115**, 16200–16210; b) S. Tang and J. Zhang, *Journal of Computational Chemistry*, 2012, **33**, 1353–1363; c) Y. Duan, Y. Geng, H. Li, J. Jin, Y. Wu, and Z. Su, *Journal of Computational Chemistry*, 2013, **34**, 1611–1619.
25. A. Gupta, A. Ali, A. Bilic, M. Gao, K. Hegedus, B. Singh, S. E. Watkins, G. J. Wilson, U. Bach, R. A. Evans, *Chem. Commun.*, 2012, **48**, 1889–1891.
26. M. J. Frisch, G. W. Trucks, H. B. Schlegel, G. E. Scuseria, M. A. Robb, J. R. Cheeseman, G. Scalmani, V. Barone, B. Mennucci and G. A. Petersson, et al., Gaussian 09, Revision B.01, Gaussian, Inc., Wallingford, CT, 2010.
27. A. D. Becke, *J. Chem. Phys.*, 1993, **98**, 5648–5652; b) A. D. Becke, *J. Chem. Phys.*, 1996, **104**, 1040–1046.
28. C. T. Lee, W. T. Yang and R. G. Parr, *Phys. Rev. B*, 1988, **37**, 785.
29. E. G. Hohenstein, S. T. Chill, and C. D. Sherrill, *J. Chem. Theory Comput.*, 2008, **4**, 1996–2000; V. S. Bryantsev, M. S. Diallo, A. C. T. Duin, and W. A. Goddard III, *J. Chem. Theory Comput.*, 2009, **5**, 1016–1026.
30. S. Miertuš, E. Scrocco and J. Tomasi, *J. Chem. Phys.*, 1981, **55**, 117–129.

31. M. Cossi, V. Barone, R. Cammi and J. Tomasi, *Chem. Phys. Lett.*, 1996, **255**, 327–335.
32. a) N. M. O'Boyle, A. L. Tenderholt and K. M. Langner, *J. Comp. Chem.* 2008, **29**, 839–845; b) R. Dennington, T. Keith and J. Millam, GaussView, Version 5, Semichem Inc., Shawnee Mission KS, 2009.
33. F. S. Mancilha, B. A. D. Neto, A. S. Lopes, Jr. P. F. Moreira, F. H. Quina, R. S. Gonçalves, and J. Dupont, *Eur. J. Org. Chem.* 2006, **21**, 4924–4933.
34. S. Kato, T. Matsumoto, T. Ishii, T. Thiemann, M. Shigeiwa, H. Gorohmaru, S. Maeda, Y. Yamashita and S. Mataka, *Chem. Commun.*, 2004, 2342–2343.
35. I. K. Moon, J.W. Oh, N. Kim, *J. Photochem. and Photobio. A: Chemistry*, 2008, **194**, 351.
36. G. Saikia and P. K. Iyer, *J. Org. Chem.* 2010, **75**, 2714.
37. a) S. H. Kim, I. Cho, M. K. Sim, S. Park and S. Y. Park, *J. Mater. Chem.*, 2011, **21**, 9139; b) D. P. Hagberg, T. Marinado, K. M. Karlsson, K. Nonomura, P. Qin, G. Boschloo, T. Brinck, A. Hagfeldt and L. Sun, *J. Org. Chem.* 2007, **72**, 9550.
38. Jr. D. W. Price and J. M. Tour, *Tetrahedron*, 2003, **59**, 3131–3156.
39. D. Sahu, C. Tsai, H. Wei, K. Ho, F. Chang and C. Chu, *J. Mater. Chem.*, 2012, **22**, 7945–7953.
40. a) J. Sung, P. Kim, Y. O. Lee, J. S. Kim, and D. Kim, *J. Phys. Chem. Lett.* 2011, **2**, 818–823; b) U. Subuddhi, S. Haldar, S. Sankararaman and A. K. Mishra, *Photochem. Photobiol. Sci.*, 2006, **5**, 459–466.
41. S. Cai, X. Hu, Z. Zhang, J. Su, X. Li, A. Islam, L. Han and H. Tian, *J. Mater. Chem. A*, 2013, **1**, 4763–4772; b) S. Cai, G. Tian, X. Li, J. Su and H. Tian, *J. Mater. Chem. A*, 2013, **1**, 11295–11305.

42. V. Rajgopal, A. Mahipal Reddy and V. Jayathirtha Rao, *J. Org. Chem.*, 1995, **60**, 7966–7973.
43. V. Rajgopal, V. Jayathirtha Rao, G. Saroja and A. Samanta, *Chem. Phys. Lett.*, 1997, **270**, 593–598.
44. U. Srinivas, P. A. Kumar, K. Srinivas, K. Bhanuprakash and V. Jayathirtha Rao, *J. Struct. Chem.*, 2012, **53**, 851–865.
45. a) A. Baheti, P. Tyagi, K. R. J. Thomas, Y.C. Hsu and J. T. Lin, *J. Phys. Chem. C*, 2009, **113**, 8541-8547; b) Y. J. Chang , T. J. Chow, *Tetrahedron*, 2009, **65**, 4726-4734.
46. C. C. Wu, T. L. Liu, W. Y. Hung, Y. T. Lin, K. T. Wong, R. T. Chen, Y. M. Chen, Y. Y. Chien, *J. Am. Chem. Soc.* 2003, **125**, 3710–3711.
47. J. Cheng, C. Lin, P. T. Chou, A. Chaskar, K. T. Wong, *Tetrahedron*, 2011, **67**, 734-739.
48. Wang, Q. Xiao, and J. Pei, *Org.Lett.* 2010, **12**, 4164-4167.
49. a) K. D. Belfield , S. Yao, M. V. Bondar, *Adv. Polym. Sci.*, 2008, **213**, 97-156; b) J. R. Lakowicz, Principles of fluorescence spectroscopy. 3rd ed. Springer; 2006.
50. a) K. R. J. Thomas, J. T. Lin, M. Velusamy, Y. T. Tao and C. H. Chuen, *Adv.Funct.Mater.*, 2004, **14**, 83-90; b) G. Qian, B. Dai, M. Luo, D. Yu, J. Zhan, Z. Zhang, D. Ma, and Z. Y. Wang, *Chem. Mater.*, 2008, **20**, 6208–6216.
51. P. Singh, A. Baheti, K.R. J. Thomas, C.P. Lee, K.C. Ho, *Dyes and Pigments*, 2012, **95** 523-533.
52. a) D. Jacquemin, E. A. Perpéte, G. E. Scuseria, I. Ciofini and C. Adamo, *J. Chem. Theory Comput.* 2008, **4**, 123-135; b) E. G. Hohenstein, S. T. Chill and C. D. Sherrill, *J. Chem. Theory Comput.*, 2008, **4**, 1996–2000.

53. V. S. Bryantsev, M. S. Diallo, A. C. T. van Duin, and W. A. Goddard III, *J. Chem. Theory Comput.*, 2009, **5**, 1016–1026.
54. a) R. E. Martin and F. Diederich, *Angew. Chem. Int. Ed.* 1999, **38**, 1350 - 1377; b) J. Xia, M. Zhou, S. Sun, G. Wang, P. Song, M. Ge, *Dyes and Pigments*, 2014, **103**, 71-75.
55. M. Ananth Reddy, A. Thomas, K. Srinivas, V. Jayathirtha Rao, K. Bhanuprakash, B. Sridhar, A. Kumar, M. N. Kamalasanan and R. Srivastava, *J. Mater. Chem.*, 2009, **19**, 6172–6184.
56. a) B. M. Wong and J. G. Cordaro, *J. Phys. Chem. C*, 2011, **115**, 18333–18341; b) B. G. Janesko, *J. Chem. Phys.*, 2011, **134**, 184105.
57. D.M. De Leeuw, M.M.J. Simenon, A.R. Brown, R.E.F. Einerhand, *Syn.Met.*, 1997, **87**, 53-59; b) H. Wang, J. Gao, L. Gu, J. Wan, W. Wei and F. Liu, *J. Mater. Chem. A*, 2013, **1**, 5875–5885.
58. B. Walker, C. Kim, T-Q. Nguyen, *Chem.Mater.*, 2011, **23**, 470–482.

Figures

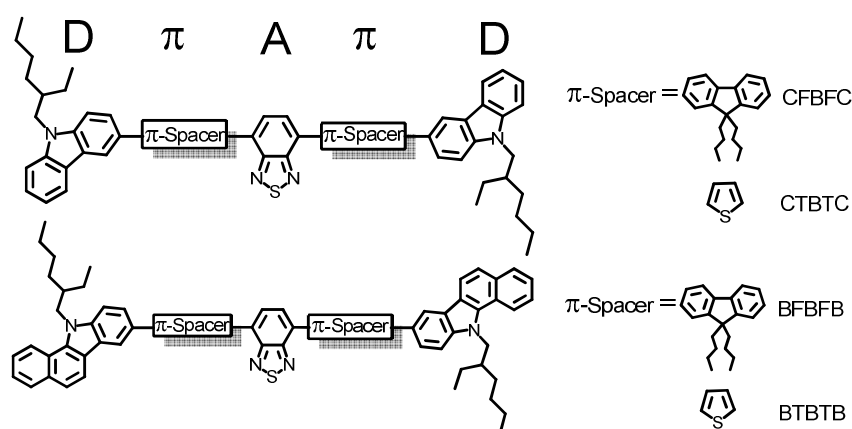
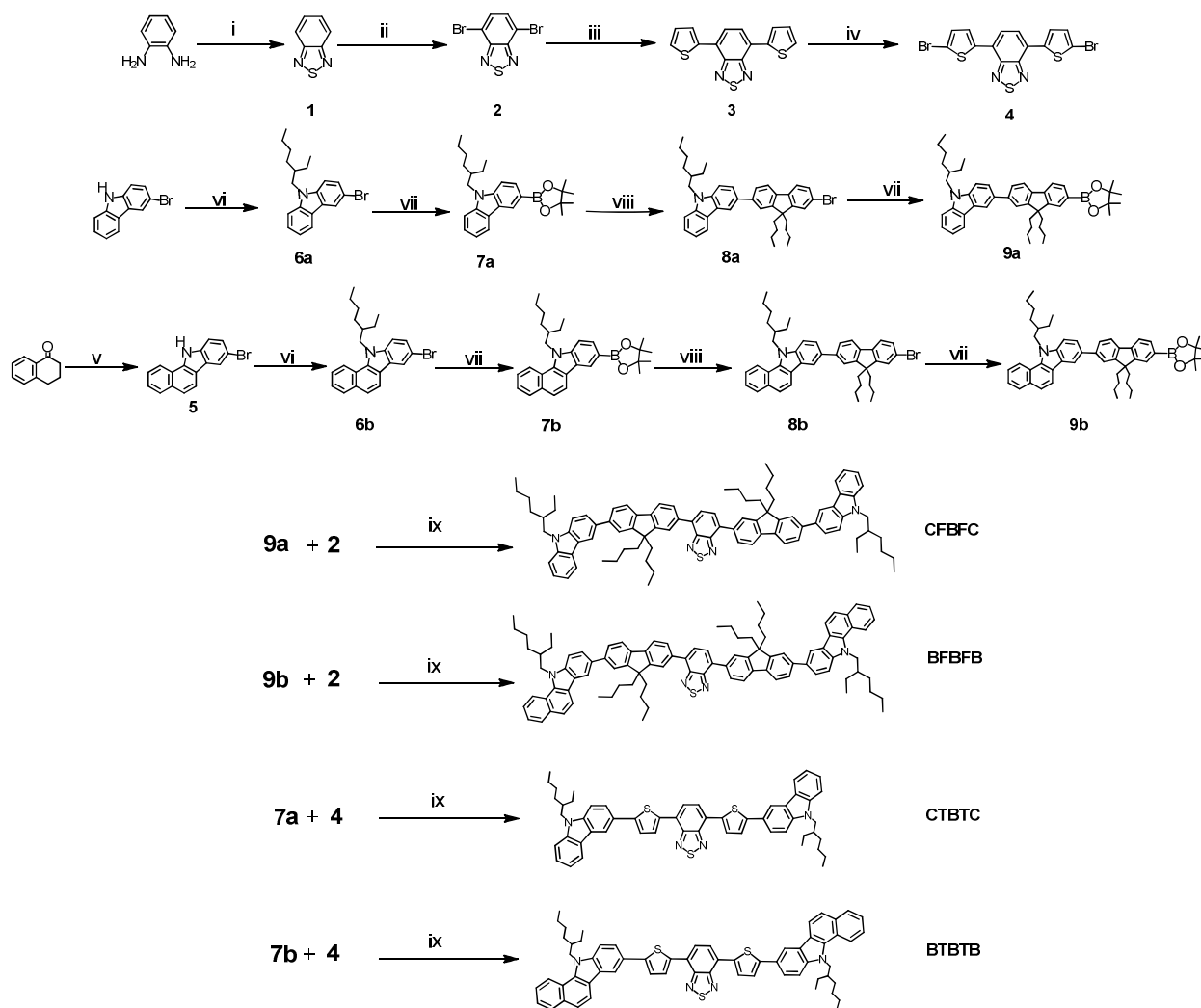


Fig. 1 Molecular structures of the dyes studied in this work.



Reagents and conditions

i) SOCl_2 , Et_3N , DCM; ii) Br_2 , 47% HBr, reflux; iii) 2-tributylstannyl thiophene, $\text{Pd}(\text{Ph}_3)_4$, toluene; iv) N-Bromosuccinimide, CHCl_3 , 48h; v) p-bromophenylhydrazine hydrochloride, AcOH (cat), EtOH, 80°C ; vi) 10 mol% tetrabutyl ammonium iodide, 50% NaOH, 80°C vii) n-BuLi, 2-isopropoxy-4,4,5,5-tetramethyl-1,3,2-dioxaborolane, THF, -78°C , 2h then rt; viii) 2,7-dibromo-9,9-dibutyl-9H-fluorene, $\text{Pd}(\text{Ph}_3)_4$, toluene / 2M K_2CO_3 ; ix) $\text{Pd}(\text{Ph}_3)_4$, 18-crown-6, toluene / 2M K_2CO_3 .

Scheme 1 Synthetic route for the preparation of target dyes

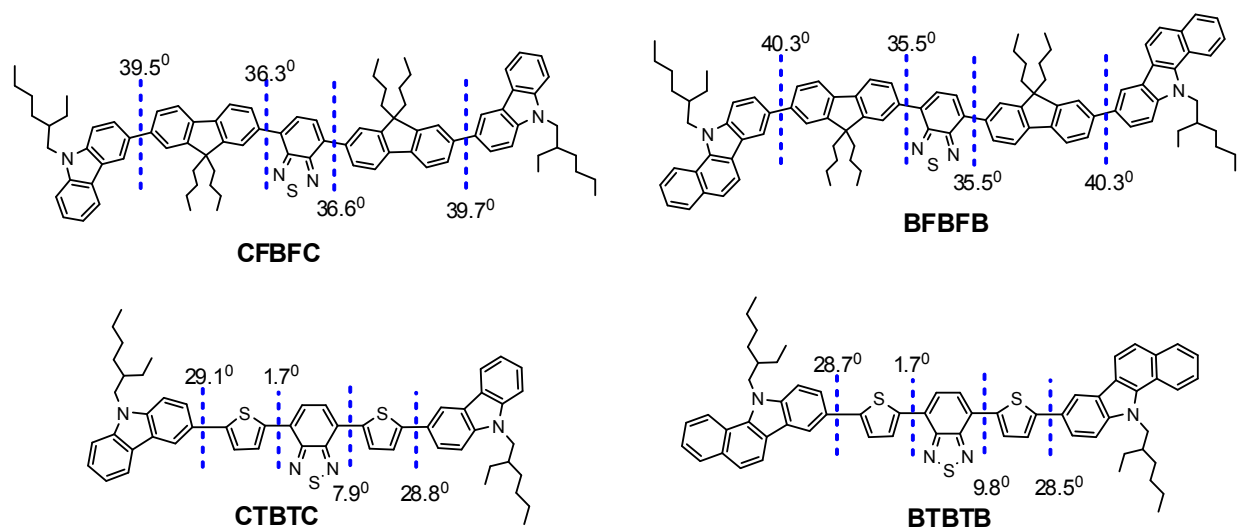


Fig. 2 Computed interplanar angles in local ground state between the different aryl segments of the dyes.

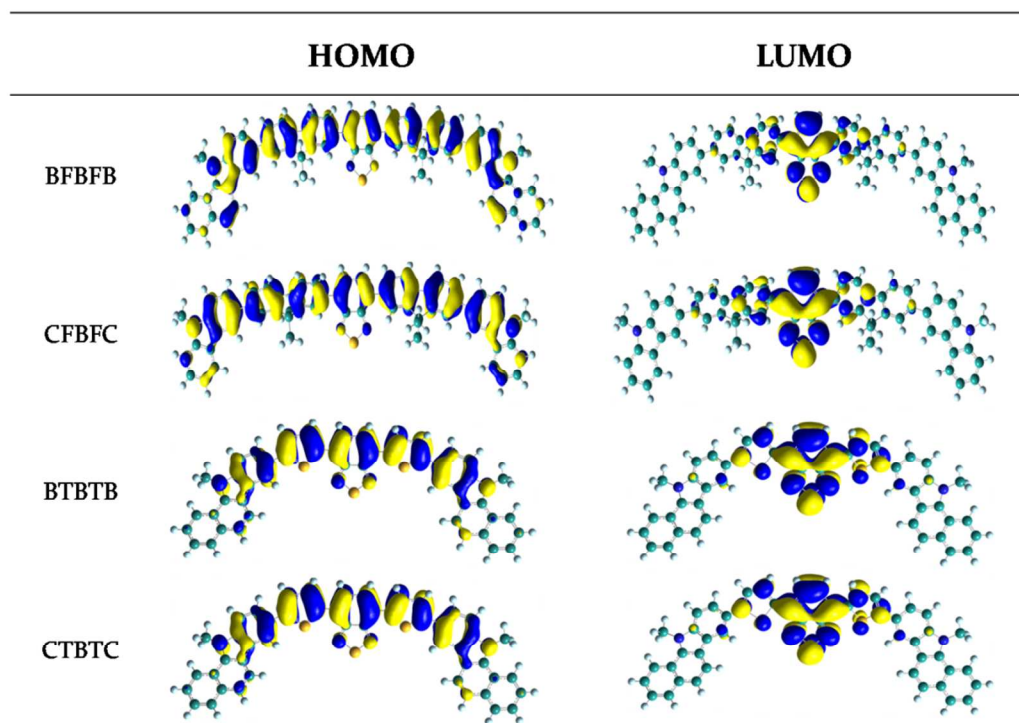


Fig. 3 Computed isodensity (0.02) surfaces of the HOMO and LUMO of the target molecules.

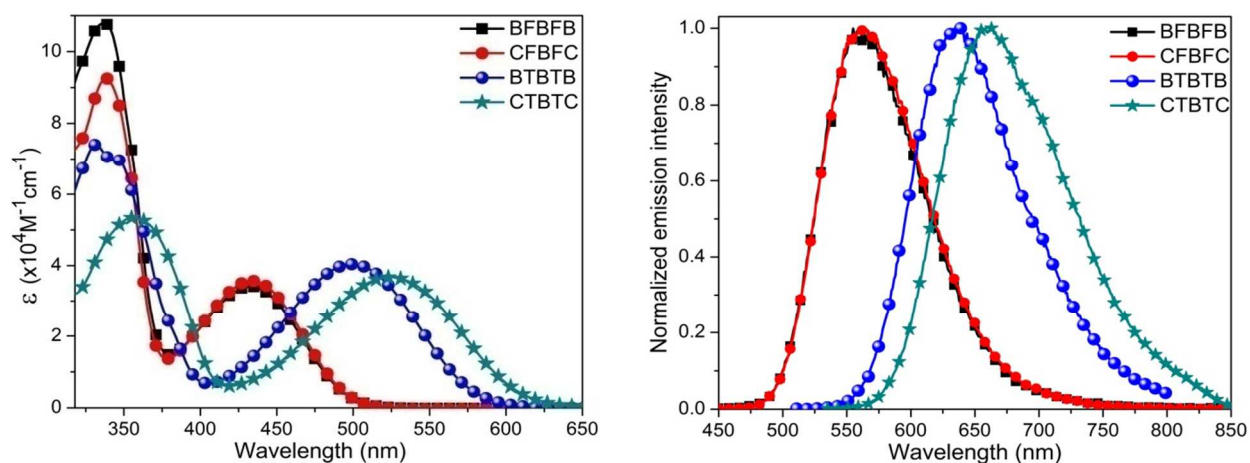


Fig. 4 UV-Vis absorption and emission spectra of dyes recorded in chloroform.

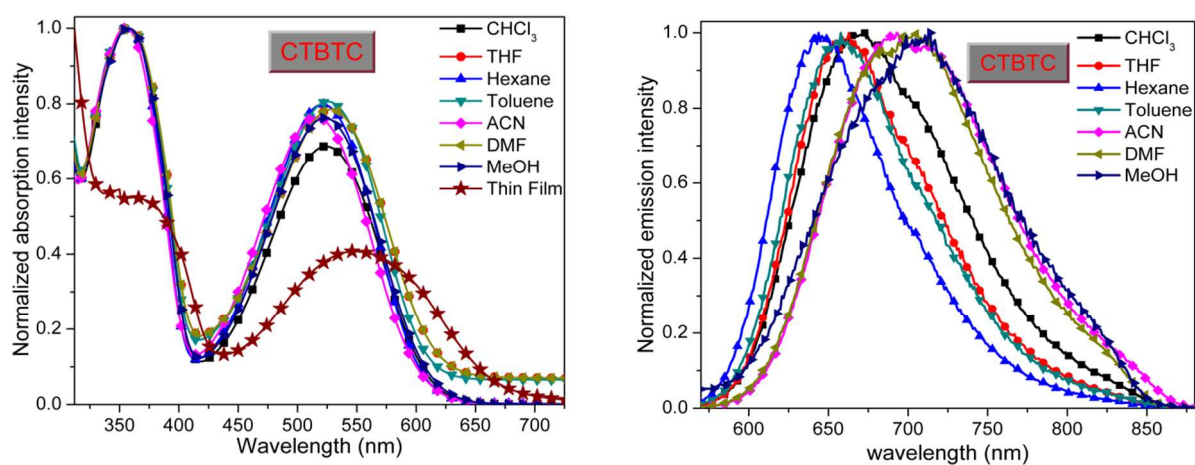


Fig. 5 Solvatochromism observed from UV-vis absorption and emission spectra of CTBTC recorded in various solvents. (for remaining dyes see ESI)

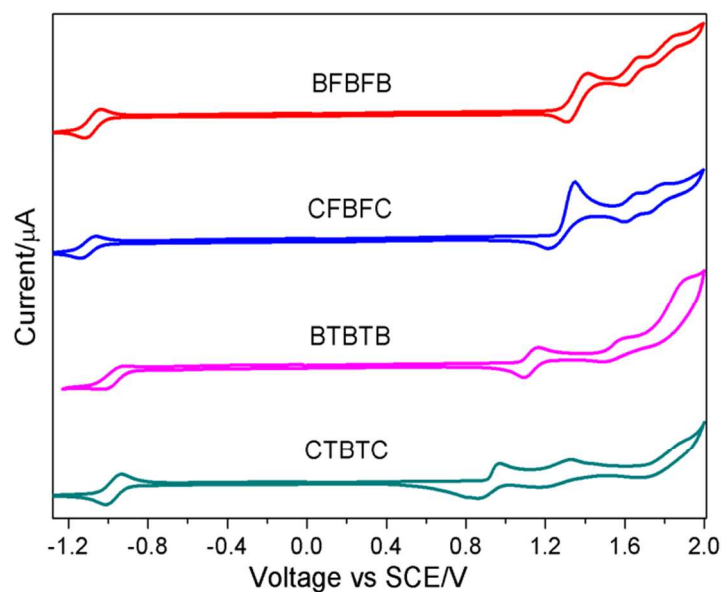


Fig. 6 Cyclic voltammograms of the dyes recorded in DCM.

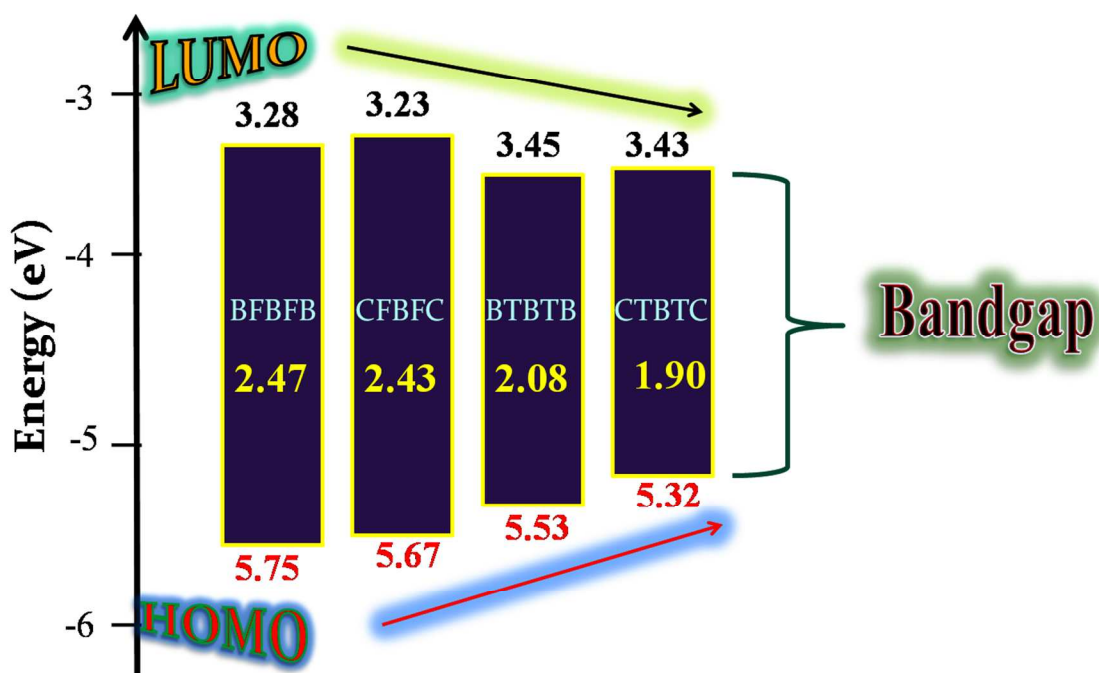


Fig. 7 Schematic representation of band gap reduction estimated from the electrochemical data.

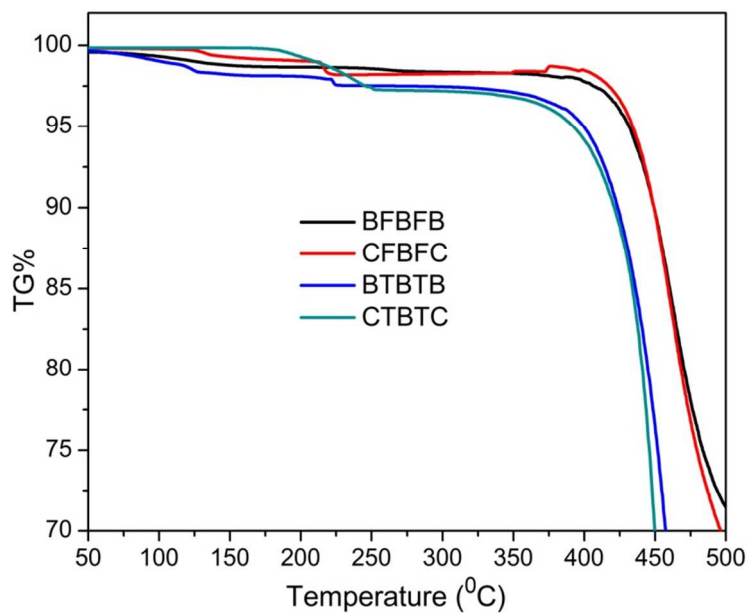


Fig. 8 TGA thermograms measured at a heating rate of 10 °C/min under N₂ atmosphere.

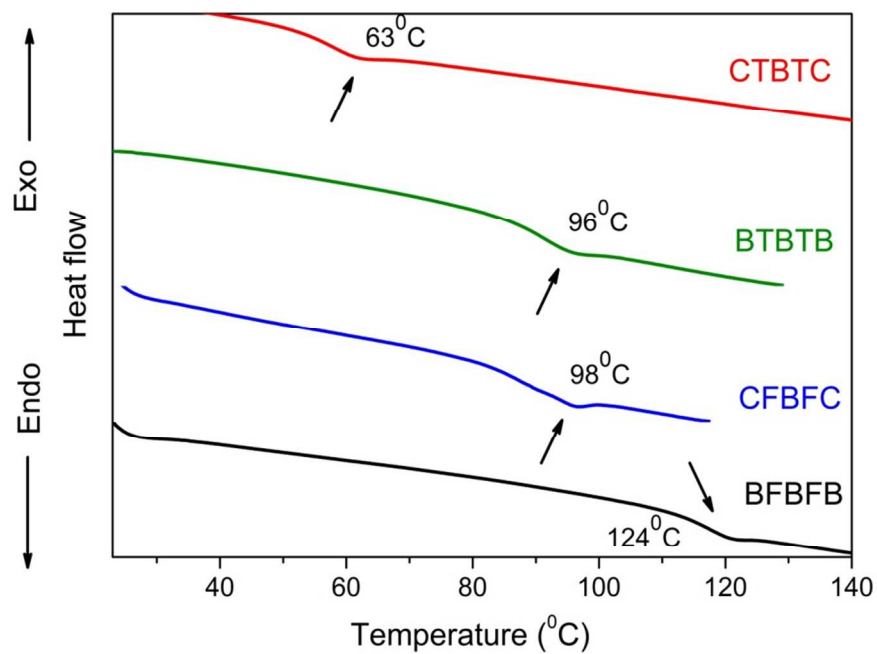


Fig. 9 DSC traces of the dyes recorded at a heating rate of 10 °C min⁻¹.

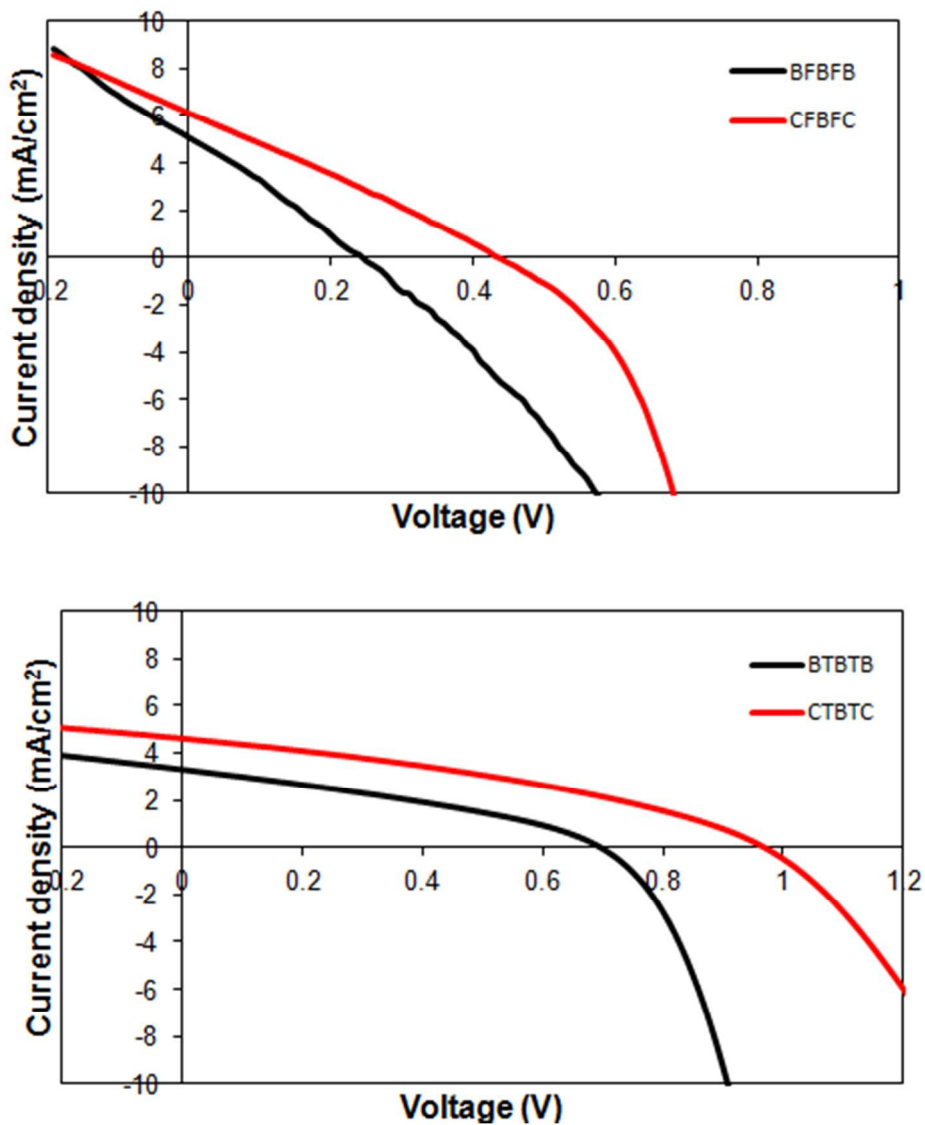


Fig. 10 Characteristic current density versus voltage (J - V) curves for best BHJ devices based on **BFBFB** & **CFBFC** (upper) and **BTBTB** & **CTBTC** (lower) in blends with PC₆₁BM under simulated sunlight (100 mW cm^{-2} AM 1.5G). Device Structure is: ITO/PEDOT: PSS (38 nm)/Active layer/Ca (20 nm)/Al (100 nm).

Table 1 Optical properties and thermal analysis data of the dyes.

Dye	$\lambda_{\text{abs}}^{\text{a}}$ (nm)	ϵ ($\text{M}^{-1}\text{cm}^{-1}$)	$\lambda_{\text{flu}}^{\text{a}}$ (nm)	$\lambda_{\text{abs}}^{\text{b}}$ film	Stokes shift (cm^{-1})	$E_{\text{g, opt}}^{\text{c}}$ (eV)	T_{d} ($^{\circ}\text{C}$)	T_{m} ($^{\circ}\text{C}$)	T_{g} ($^{\circ}\text{C}$)
BFBFB	433 337	34,063 1,07,859	563	447	5333	2.36	433	270	121
CFBFC	434 338	35,653 92,477	563	447	5280	2.30	435	215	98
BTBTB	499 332	40,343 74,029	639	521	4391	1.95	376	192	96
CTBTC	524 356	36,706 53,401	663	544	4001	1.85	372	173	63

^a absorption and emission spectra in chloroform in the concentration of 1×10^{-5} M at ambient temperature.

^b measured in thin film state.

^c estimated from the onset absorption spectra of the compounds in thin film state.

T_{d} - decomposition temperature (corresponding to 5% weight loss).

T_{m} - melting point of the compounds.

T_{g} - glass transition temperature and values are from the second heating scan.

Table 2 Comparison of the experimental optical properties with the theoretical data.

Dye	$\lambda_{\text{max}}^{\text{a}}$ (nm)	M06-2X (Chloroform)			$\mu_{\text{gs}}^{\text{b}}$	$\mu_{\text{ge}}^{\text{c}}$
		λ_{max} (nm)	f	Composition		
BFBFB	433	404 (3.07 eV)	1.61	HOMO->LUMO (54%) HOMO-2->LUMO (25%)	2.3	2.6
CFBFC	434	404 (3.07 eV)	1.54	HOMO->LUMO (65%) HOMO-2->LUMO (25%)	2.1	2.5
BTBTB	499	500 (2.48 eV)	1.37	HOMO->LUMO (90%) HOMO-2->LUMO (5%)	2.3	3.1
CTBTC	524	503 (2.47 eV)	1.19	HOMO->LUMO (92%) HOMO-2->LUMO (4%)	2.3	3.1

^a recorded in chloroform (1×10^{-5} M solution).

^b dipole moment of the dyes in ground state (debye units) obtained from B3LYP/6-311g(d,p) level.

^c transition dipole moment of the dyes (debye units) obtained from M06-2X/6-311g(d,p) level.

Table 3 Comparison of electrochemical data measurements vs. values obtained from DFT

Dye	$E_{\text{onset}}^{\text{a}}$ (V)		HOMO ^b (eV)	LUMO ^b (eV)	$E_{\text{g, ele}}^{\text{c}}$ (eV)	DFT ^d		Band Gap ^e (eV)
	oxd	red				HOMO (eV)	LUMO (eV)	
BFBFB	1.35	-1.12	-5.75	-3.28	2.47	-5.25	-2.55	2.70
CFBFC	1.27	-1.17	-5.67	-3.23	2.44	-5.24	-2.53	2.70
BTBTB	1.13	-0.95	-5.53	-3.45	2.08	-5.00	-2.67	2.33
CTBTC	0.92	-0.97	-5.31	-3.43	1.90	-4.97	-2.66	2.32

^a measured in CH_2Cl_2 with 0.1 M Tetrabutylammonium perchlorate (TBAPC) as supporting electrolyte with a scan rate between 50 mVs^{-1} .

^b deduced from the formula $\text{HOMO} = -(4.4 + E_{\text{ox}})$ and $\text{LUMO} = -(4.4 + E_{\text{red}})$

^c bandgap obtained from electrochemical data

^d computed values from B3LYP/6-311G (d, p) level

^e band gap obtained from theoretical data.

Table 4 Comparative BHJ solar cells performances

Dye	Blend film thickness ^a (1:1@3000 rpm)	V _{oc} (mV)	J _{sc} (mA/cm ²)	FF	Efficiency ^b (η%)
BFBFB	64	250 ± 30	5.09 ± 0.4	0.23 ± 0.04	0.30 ± 0.08
CFBFC	66	430 ± 20	6.13 ± 0.6	0.26 ± 0.03	0.71 ± 0.15
BTBTB	62	691 ± 30	3.30 ± 0.3	0.32 ± 0.02	0.76 ± 0.07
CTBTC	63	960 ± 20	4.63 ± 0.2	0.34 ± 0.03	1.62 ± 0.06

^a BHJ devices with specified weight ratio. Device structure is ITO/PEDOT: PSS (38 nm)/active layer/Ca (20 nm)/Al (100 nm) with active layer thickness of about 65 nm.

^b Average value based on 10 devices.

Graphical Abstract

